Research Article

Geochemistry, Geophysics, Geosystems
DOI 10.1002/2016GC006504

Late Cenozoic tephrostratigraphy offshore the southern Central American Volcanic Arc:
2. Implications for magma production rates and subduction erosion

Schindlbeck, J.C.[1], Kutterolf, S.[1], Freundt, A.[1], Straub, S.M.[2], Vannucchi[3,4], P., Alvarado, G.E. [5,6]

[1]GEOMAR Helmholtz Centre for Ocean Research Kiel, 24148 Kiel, Germany

[2]Lamont-Doherty Earth Observatory/Columbia University, Palisades NY 10964, USA

[3]Royal Holloway, University of London, Egham, Surrey, TW20 OEX, UK

[4]Universita' degli Studi di Firenze, Via La Pira 4, 50121 Firenze, Italy

[5]Instituto Costarricense de Electricidad, Apdo. 10032, 1000 San José, Costa Rica

[6]Centro de Investigaciones Geológicas, Apdo. 35-2060, Universidad de Costa Rica, San José, Costa Rica

Corresponding author: Julie C. Schindlbeck (jschindlbeck@geomar.de)

Key Points:

- Central American Volcanic Arc volcanism
- Magma Production rates
- Sedimentation rates offshore Costa Rica and Nicaragua

Received: Jun 23, 2016; Revised: Sep 20, 2016; Accepted: Sep 21, 2016

Abstract

Pacific drill sites offshore Central America provide the unique opportunity to study the evolution of large explosive volcanism and the geotectonic evolution of the continental margin back into the Neogene. The temporal distribution of tephra layers established by tephrochonostratigraphy in Part 1 indicates a nearly continuous highly explosive eruption record for the Costa Rican and the Nicaraguan volcanic arc within the last 8 M.y.

The widely distributed marine tephra layers comprise the major fraction of the respective erupted tephra volumes and masses thus providing insights into regional and temporal variations of large-magnitude explosive eruptions along the southern Central American Volcanic Arc (CAVA). We observe three pulses of enhanced explosive magmatism between 0-1 Ma at the Cordillera Central, between 1-2 Ma at the Guanacaste and at >3 Ma at the Western Nicaragua segments. Averaged over the long-term the minimum erupted magma flux (per unit arc length) is ~0.017 g/ms.

Tephra ages, constrained by Ar-Ar dating and by correlation with dated terrestrial tephras, yield time-variable accumulation rates of the intercalated pelagic sediments with four prominent phases of peak sedimentation rates that relate to tectonic processes of subduction erosion. The peak rate at >2.3 Ma near Osa particularly relates to initial Cocos Ridge subduction which began at 2.91±0.23 Ma as inferred by the 1.5 M.y. delayed appearance of the OIB geochemical signal in tephras from Barva volcano at 1.42 Ma. Subsequent tectonic re-arrangements probably involved crustal extension on the Guanacaste segment that favored the 2-1 Ma period of unusually massive rhyolite production.

1 Introduction

The accumulation of sediments in ocean basins records processes that control the flux of sediments from their sources. Interpretation of the marine sediment succession requires

high-resolution timing of their emplacement. Offshore Central America, such age constraints are provided by the tephrostratigraphic record of large magnitude, high intensity explosive eruptions at the southern Central American Volcanic Arc (CAVA) that we have established in Part 1. Here we investigate consequences for the two main types of deposits: pyroclastic deposits and marine sediments.

For each of the large explosive eruptions, the tephra volume on the Pacific seafloor represents a major fraction of total volume. Marine tephra layers often provide a first assessment of eruption magnitudes for periods of explosive volcanism that are poorly exposed in the terrestrial environment. Temporal variations in these volumes can serve as a first-order proxy for time-variations of the erupted volcanic material at the arc and understanding these past changes may help to understand future developments. Previous studies examined therefore the budget of material input and output at the CAVA [e.g., *Carr et al.,* 2007; *Kutterolf et al.,* 2008b] through Late Pleistocene to Holocene times. *Carr* [1984] and *Carr et al.* [1990, 2007] calculated magma fluxes over time by converting the volumes of the volcanic edifices on land into magma masses. This work was later complemented by magma masses derived from widely dispersed tephras from Plinian eruptions which can account for almost half of the total erupted mass [*Kutterolf et al.*, 2008b]. They presented variations of magma fluxes per volcanic center, whereas *Freundt et al.* [2014] summarized the temporal changes for each tectonic segment. While these previous studies have been limited to the Late Pleistocene and Holocene, the tephra record exploited here facilitates estimates of magma fluxes and eruptive magnitudes back through Pliocene times.

Pelagic and hemipelagic clastic sedimentation on the continental slope and across the subduction trench onto the incoming plate are controlled by morphologies of the submarine slope, the subducting plate, and the continental hinterland. Morphology, in turn, is controlled by tectonic processes. The major tectonic processes in southern Central America are

subduction erosion and the closure of the Caribbean-Pacific gateway. Subduction erosion involves local uplift and subsidence at the continental slope, and such erosion is particularly efficient where seamounts are subducted. Erosive margins and their opposite, accretionary margins, are defined based on the transfer of material occurring at the forearc: erosive margins are characterized by net removal of upper plate material occurring at the front or at the base of the forearc, accretionary margins accumulate the sediment from the incoming plate at the front of the forearc or by underplating, leading to a net growth of the margin [*von Huene and Scholl,* 1991; *Clift and Vannucchi,* 2004]. The removal of material at erosive subduction zones leads to subsidence of the margin itself [e.g., *Lallemant et al.,* 1996] as well as deepening of the forearc basin, which, in case of high sedimentation flux, can be rapidly filled with sediments [e.g., *Vannucchi et al.,* 2016]. Sedimentation rates can therefore be a proxy for the rate of subduction erosion [*Vannucchi et al.,* 2003]. Offshore Central America drilling and seismic data indicate long-term subsidence of the continental slope and therefore active and long-lived subduction erosion from Guatemala to Costa Rica, temporally enhanced due to variable roughness of the incoming plate. In Southern Costa Rica, the Cocos Ridge collision off Osa Peninsula has been also associated with uplifting of the hinterland – i.e. Fila Costeña and Cordillera de Talamanca - [e.g., *Ranero and von Huene,* 2000; *Ranero et al.,* 2000; *Vannucchi et al.,* 2001, 2003, 2004; 2013; *Clift and Vannucchi,* 2004; *Morell et al.,* 2012]. Though, recent detrital thermochronology on the southern Costa Rica forearc sediments reveals that the uplift of the Fila Costeña and Cordillera de Talamanca is not directly correlated with the onset of the Cocos Ridge subduction [*Vannucchi et al.,* accepted]. The basal part of the upper plate in the fore-arc of Costa Rica, which is subject of subduction erosion, is characterized by accreted Cretaceous OIB-material [e.g., *Clift et al.,* 2005; *Hauff et al.,* 2000]. When such material is transferred into the sub-arc melting zone the generated melts can potentially inherit traces of that OIB composition. The temporal variation of geochemical compositions of the arc-volcanic products thus may help to track changes in

subduction erosion through time. Here we determine changes in sedimentation rates on the slope and incoming plate and changes in geochemical compositions of arc tephras since the Pliocene, and discuss how these changes relate to time-varying tectonic processes.

2 Geological background

The CAVA extends from Panama to Guatemala and parallels the deep-sea Middle American Trench (MAT) at a distance of 150–200 km (Fig. 1), which is the best-studied erosive subduction margin [*Ranero and von Huene,* 2000; *Vannucchi et al.,* 2001, 2003, 2004, 2013; *Straub et al.,* 2015]. The CAVA is the result of the subduction of the oceanic Cocos plate beneath the Caribbean plate at a convergence rate of 70–90 mm/a [*Barckhausen et al.,* 2001; *DeMets,* 2001] (Fig. 1A). The Cocos plate has been formed at two spreading centres, the East Pacific Rise and the Cocos-Nazca Spreading Center and it is strongly influenced by the Galápagos hotspot volcanism. The most prominent feature on the Cocos plate is the aseismic Cocos Ridge (Fig. 1A) representing the Galápagos hotspot track that subducts near Osa Peninsula, Costa Rica. This ridge is flanked northward by numerous seamounts that are subducted off central Costa Rica, and southern Nicaragua [e.g., *Hühnerbach et al*., 2005; *Dinc et al.*, 2010] (Fig. 1A).

The CAVA is subdivided into tectonic segments by Caribbean tectonic structures as well as by strike-slip tectonics caused by strain partitioning between the forearc and the backarc [*Morgan et al.,* 2008]. From Costa Rica to Guatemala the slab dip varies between 40° and 75° with Nicaragua having the steepest angle [*Cruciani et al.,* 2005; *Protti et al.,* 1995; *Syracuse and Abers,* 2006]. Dextral strike-slip tectonics divide the volcanic front into ten segments [*Carr et al.,* 1984; *DeMets,* 2001]. Herein we focus on the Costa Rican and Nicaraguan segments; the Cordillera Central (CCS), the Guanacaste (GCS), the Eastern Nicaragua (ENS) and the Western Nicaragua (WNS) segments (Fig. 1A).

Subduction-related volcanism in Costa Rica started at least since the Upper Cretaceous and reached more extensive calc-alkaline and tholeiitic activity between the Oligocene and Quaternary [e.g., *Alvarado and Carr,* 1993; *Tournon and Alvarado,* 1997]. Numerous large explosive eruptions occurred at least since the Miocene [e.g., *Jordan et al.,* 2007a,b; *Vogel et al.,* 2004; *Alvarado and Gans,* 2012] and are associated with Orosí, Rincón de la Vieja, Miravalles, Tenorio, Arenal, Platanar, Poás, Barva, Irazú, Turrialba volcanoes and their associated pre-caldera stages as well as the known Quaternary and Pliocene Cañas Dulces and Guayabo calderas in Guanacaste (Fig. 1A). The Upper Pleistocene to Holocene record of widespread tephra layers from the modern volcanic front in Nicaragua has been intensively studied [c.f. *Bice*, 1985; *Kutterolf et al.,* 2007a] and originated mostly from the Malpaisillo Caldera, Apoyo Caldera, Masaya Caldera, Chiltepe volcanic complex, and Cosigüina volcano (Fig. 1A). Less is known about the Pliocene and Miocene volcanic arcs in Nicaragua that are displaced up to 100 km towards the east as they formed prior to a major slab rollback [*Barckhausen et al.,* 2001; *DeMets,* 2001] between the Miocene and Pliocene [*Ehrenborg,* 1996]. This older Coyol arc (Fig. 1A) hosts rhyolitic calderas (*Ehrenborg,* 1996) and produced numerous ignimbrites that feature geochemical characteristics inherited by contamination with continental crust [*Jordan et al.,* 2007a,b].

3 Sedimentation rates offshore Costa Rica and Nicaragua

Our database encompasses ~650 ash horizons in the 18 drill sites, including primary ash beds and slightly reworked ash that retained its compositional integrity and stratigraphic position, 430 of these originated at the CAVA while the other ashes stem from the Galápagos hotspot and from Cocos Island (in total 220 ash beds) [*Schindlbeck et al.,* 2015, sub., part 1]. These correlations are mainly based on major and trace element glass compositions as well as on structural and lithological characteristics, stratigraphic relationships and age.

As discussed in Part 1 directly dated and unambiguously correlated ash layers provide additional timelines for the marine records that improve the age models derived from biostratigraphic data and/or palaeomagnetic ages [*Kimura et al.,* 1997; *Harris et al.,* 2013; *Mix et al.,* 2003; *Pisias et al.,* 1995]. Ages for marine tephra layers have been obtained by correlation of marine tephra layers with dated deposits on land and by direct Ar/Ar age dating of feldspars in selected marine samples. These time markers improve the precision of age-dependent apparent marine sedimentation rates calculated from the thicknesses of pelagic and hemipelagic sediments intercalated between these time markers. The sedimentation rates between two age anchors are average values since we apply linear interpolation. In Part 1 we have used these sedimentation rates to obtain ages for all other ash beds that had not been dated otherwise.

Figure 2 illustrates sedimentation rates for selected cores of slope and incoming plate sites. Overall, we observe marine sedimentation rates of 5–200 m/M.y. on the incoming plate and 3-950 m/M.y. on the continental slope offshore the southern CAVA. The apparent sedimentation rates can vary with depth at both deep marine environments (Fig. 2), which may be due to variable amount of terrigenous detritus defining hemiplegic versus pelagic sedimentation, and to tectonic controls that regulate the temporal capacity of sediment sources and sinks. In the following we describe the sedimentation rates on the incoming plate and on the continental slope in detail.

3.1. On the incoming plate

The refined sedimentation rates for Sites 1241, 1242, U1414, and U1381 (Figs 2A, B, 3a and *Baxter et al.* [submitted]) remain close to those established by the shipboard parties [*Harris et al.,* 2013; *Mix et al.,* 2002]. However, for Site 1039 [*Kimura et al.,* 1997] the discrepancies to the shipboard data are larger since 20 ages of tephra correlations and two

Ar/Ar datings provide the basis for a more detailed age model. Nine tephra ages within the sediments below the decollement of Site 1040 also improve the respective age model.

Sedimentation was not monotonous through time on the entire incoming plate (Fig. 3a) and notably hiati lasting several million years are observed at Sites U1381 (1.5 to 8 Ma) and 1242 (2 to 12 Ma). Late Pleistocene hemipelagic sedimentation rates reach high values at Sites 1039 (83 m/M.y.), 1040 (75 m/M.y.; below decollement), U1414 (200 m/M.y.), U1381 (150 m/M.y.). Toward the Early Pleistocene, when these sites were farther away from the trench, sedimentation rates at these sites typically decrease rapidly down to 5 m/M.y., the average for Pacific pelagic sedimentation in this region [*Schindlbeck et al.,* 2015].

Nevertheless, we observe some exceptions on the incoming plate during the Neogene and Late Pleistocene. The Neogene sediment accumulation rates at Site 1039 (13-43 m/M.y.), offshore Nicoya, Sites 1242 (~45 m/M.y.) and U1414 (14-21 m/M.y.), offshore Osa on the eastern and western Cocos Ridge flanks, and Site 1241 (29-68 m/M.y.), on the crest of the Cocos Ridge, are much higher than the values of 1 to 5 m/M.y., which are expected from pelagic sediment of an open ocean deep sea environment (according to the kind of ooze or clay that is deposited) [e.g., *Rothwell,* 2005; *Hüneke and Mulder,* 2011]. However, Site 844 (2.5-6.5 m/M.y.; until the Late Miocene), and to some extent Site U1381 (~5 M.y.; for the Late to Middle Miocene), match the expected low pelagic sedimentation rates, although they are located close to the neighboring sites with higher sedimentation rates (Fig. 1).

3.2. On the continental slope

The new age models significantly change the previously published sedimentation rates [e.g., *Vannucchi et al.,* 2012; *Harris et al.,* 2013; *Kimura et al.,* 1997] for the southern Central American continental slope (Figs 2E-J, 3b). The revised Pleistocene sedimentation rates are predominantly higher than the previous values at Sites U1378, U1379, and U1380 and

alternating lower or higher at Sites 1041 and U1413, whereas the sedimentation rates are lower at Sites U1412 and 565 throughout (Figs 2F, G, 3b).

From South to North the middle to upper slope sedimentation rates decrease from 600-1000 m/M.y. offshore Osa Peninsula (Sites U1378, U1379, U1413) to 50-100 m/M.y. off Nicoya Peninsula (Sites 565, 1040, 1041) and to 30-40 m/M.y. at the Nicaraguan slope [e.g. *Kutterolf et al.,* 2008c,d]. In the Late Pleistocene to Holocene (0 to ~200 ka) sedimentation rates offshore Osa Peninsula are up to one order of magnitude higher at Site U1379 (~900 m/M.y.), Sites U1378, U1412 and U1413 (250 to 350 m/M.y.) than offshore Nicoya Peninsula (Sites 565, 1040, 1041; 38–50 m/M.y.) (Fig. 2 E-J).

Between ~1.2 Ma and 0.2 Ma the sedimentation rates at Site U1378 decrease to ~200-300 m/M.y., the same level as at Site U1379 and increase again up to 820 m/M.y. (Site U1379) and 940 m/M.y. (Site U1378) between 1.6 and 1.2 Ma. In the early Pleistocene the sedimentation rates stay constant with low values of ~70 m/M.y. at Site U1378 and high sediment accumulation at Site U1379 (~400 m/M.y.; Fig. 2I, J).

The sedimentation rates offshore Nicoya Peninsula (Site 1040, Fig. 2C) increase downward from 25 m/M.y. to ~50 m/M.y. in the early Pleistocene. For the rest of the Pleistocene and most of the Pliocene the sedimentation rates at the entire slope stay constant at ~50 m/M.y. offshore Nicoya, similar to the sediment accumulation at the slope off Nicaragua.

4 Explosive eruption magnitudes

4.1. Tephra volumes and magma masses

During the Upper Pleistocene, ash plumes of numerous Plinian, Phreatoplinian and ignimbrite-forming eruptions from Central America were dispersed westward at tropospheric and stratospheric heights across the Pacific [*Kutterolf et al.,* 2007a, 2008a]. The resulting marine ash layers cover areas of up to 10^6 km^2 in the Pacific Ocean and represent a major fraction of the erupted tephra volumes [*Kutterolf et al.,* 2008b]. Neither onshore nor offshore

contributions of the older, Lower Pleistocene and Pliocene, CAVA explosive volcanism have yet been volumetrically quantified.

In part 1 we established the tephrochronostratigraphy for the Late Miocene to Late Pleistocene of Costa Rica and Nicaragua by correlating 39 tephra layers with chemical fingerprinting to onshore deposits. Moreover we compared the compositions of 204 tephra beds with the systematic compositional changes along the southern CAVA to elucidate the origin of the respective, so far unknown eruptions. In this second part of our contribution, we use these correlations and ash distributions on the seafloor and on land including published isopach maps to better constrain erupted volumes of the widespread tephras and thus the magnitudes of the large eruptions that occurred at the southern CAVA during the past 8 M.y.. For most tephras of the southern CAVA, however, data on distribution on land does not exist. Nevertheless, for marine tephra layers of which we can reasonably constrain the region of origin, it is possible to estimate useful minimum tephra volumes without on-land data, because the Pleistocene-Holocene examples show that the distal, marine volume fraction typically accounts for more than half the total tephra volume [e.g., *Kutterolf et al.,* 2008b].

In order to reconstruct the original areal distribution, we have shifted the present site locations away from the arc according to the tephra age, using the plate motion vector of *De Mets* [2001] (cf. Fig. 1). Where thickness data of multiple sites were available, we drew isopachs for calculating the distribution area and respective volumes (Fig. 4). We also complement isopach maps for some late Pleistocene tephras (e.g., Tiribí Tuff (marine layer *H*) and Fontana Tephra (layer *D*)) (Fig. 4) previously made from onshore outcrops and marine gravity cores, to improve the tephra volume estimates [*Freundt et al.,* 2006; *Kutterolf et al.,* 2007a,b, 2008b; *Pérez and Freundt,* 2006; *Wehrmann et al.,* 2006] (Table S1).

Total tephra volumes are obtained by fitting straight lines to data on plots of ln [isopach thickness] versus square root [isopach area] following *Pyle* [1989] and *Fierstein and Nathenson* [1992] and integrating to infinity. Since the offshore thickness data are sparse, the shape of the distal isopachs contours can only be estimated introducing some errors into the volume calculations depending on how the data are treated during isopach construction. Nevertheless, the study by *Klawonn et al.* [2014] showed that possible errors in volume calculations, imparted by individuals' choices of contours applied to the same data set, are surprisingly low between 5 and 8%.

Where data was too scarce for this approach we followed *Legros* [2000] and calculated a minimum tephra volume by assuming the thickness at the farthest site lies on the dispersal axis, constructing a tear-drop shaped isopach with an aperture angle of 45° (an average angle for Pleistocene eruptions; e.g. *Kutterolf et al.* [2007a, 2008b]), and accounting for exponential thickness decrease. We convert tephra volume to magma mass following the procedure of *Kutterolf et al.* [2008b]. Measured average ash-particle densities are typically 2.1 g/cm^3 for felsic and 2.4 g/cm^3 for mafic marine ash beds [e.g., *Kutterolf et al.,* 2008b]. We reduce the determined total marine tephra volumes by ~30%, because the subtraction of ~40% interparticle space is partially balanced by an addition (~20%) of ash that is mixed with sediments above the distinct ash layers. Selected isopach maps (Fig. 4) and thickness versus square-root of isopach area variations (Fig. 5) illustrate the wide distribution for the investigated tephra layers and support their emplacement by eruptions of Plinian intensities. All calculated volumes are presented in the supplement Table S1. Our calculated volumes represent minimum estimations and cover often only the distal co-ignimbrite ash fall fraction of the respective ignimbrite-forming eruptions. For few of them we could integrate published ignimbrite volume estimations. Overall the determined distal tephra volumes (based on marine isopachs) for the tephra layers range from 0.32 km^3 (*s2*) up to 230 km^3 (*H*; Tiribí

Tuff). Although some of these tephras have been well-known, our estimates are often the first quantification of the respective eruption magnitudes.

4.2. Eruption magnitudes

In a next step we determine the eruption size for all eruptions with estimated volumes. While the well-known Volcanic Explosivity Index [VEI; *Newhall and Self,* 1982] measures eruption size in discrete classes, mainly based on tephra volume, the volumetric magnitude of eruptions M_V=log10(V) −4, where V [m^3] is the tephra volume [*Pyle,* 1995], has the advantage of a continuous scale. Nevertheless, VEI and M_V can be seen to be equivalent since first numeral values are the same for most eruptions [*Pyle,* 2000]. In Figure 5, the higher a curve in the graph the larger the eruption magnitude, and the shallower the slope of a curve the higher the eruption intensity, i.e. mass discharge rate and column height. Therefore all investigated CAVA eruptions had intensities and magnitudes ranging from those of the Mount St. Helens 1980 to those of the Tambora 1815 eruptions (Fig. 5). The largest known eruption of the Cordillera Central segment in Costa Rica (CCS) is the 322 ka Tiribí Tuff. Its tephra volume has previously been estimated at about 78 km^3 combining the on land ignimbrite distribution of *Pérez et al.* [2006] with offshore data of *Kutterolf et al.* [2008a,b]. The revised marine tephra distribution across ~800,000 km^2, yields 266 km^3 of erupted tephra volume composed of ~231 km^3 distal tephra volumes and 35 km^3 of proximal ignimbrite tephra volume, placing Tiribí Tuff into an eruption magnitude of M_V=~7.4. The distal, marine tephra probably contains a significant fraction of co-ignimbrite ash, which may represent a volume subequal to that of the ignimbrite [cf., *Sigurdsson and Carey,* 1989; *Kandlbauer and Sparks*, 2014], but most of the distal ash may be equivalent to the proximally up to 3 m thick Tibas Pumice fallout underlying the ignimbrite on land [*Pérez et al.,* 2006].

We have identified five widespread tephra layers (100,000 to 270,000 km^2) that probably originate from Barva volcano. These previously unknown eruptions produced minimum tephra volumes of 18 to 60 km^3 or M_V= 6.2 to 6.8, respectively, emphasizing the significance of Barva volcano for hazard assessment. Nearby Poás volcano, on the other hand, has produced much smaller eruptions in the range of 2 km^3 (M_V= 5) for each of marine tephra layers *C1* and *C2*. Marine tephra layers *K1* and *K2* yield the first size estimates (8.7 and ~3.2 km^3, M_V= 6 and 5.5) for the Upper (0.44 Ma) and Lower (0.58 Ma) Alto Palomo Tuffs [*Villegas,* 2004] from the caldera hosting the younger Platanar and Porvenir volcanoes. Another eruption of the same compositional signature (tephra layer *s12*) resulted in a tephra volume of at least 1.6 km^3 (M_V= 5.2).

A much longer eruptive history is recorded in the cores for the Guanacaste segment in northern Costa Rica (GCS), going back to at least 8 Ma, and our calculations facilitate a first systematic evaluation of the tephra volumes for this arc segment. The youngest (~3.5 ka) widespread tephra originated from Rincón de la Vieja volcano (Rincón de la Vieja Tephra; *A*) and has a volume of 1.1 km^3 (M_V= 5), which is four times the estimate of 0.25 km^3 of *Kempter* [1997], for the onshore portion alone. Five other widespread tephra layers erupted from the Rincón de la Vieja volcanic complex in the last ~300 ka (*s1, s5, s6, s7, s8*) range between 1.1 and 2.8 km^3 tephra volume (M_V= 5 to 5.5), suggesting that such eruption sizes commonly occur. Two approximately 400 ka old tephras tentatively correlated to Tenorio volcano reflect similar eruption sizes (*I*=1.8 km^3, M_V= 5.3; *s11*=1.2 km^3, M_V=5.1).

The total erupted tephra volume of the La Ese Ignimbrites (Upper and Lower La Ese Ignimbrites; ~0.6 to 0.9 Ma), erupted from the Guayabo Caldera, has previously been estimated to 5.5 km^3, based on onshore mapping [*Chiesa et al.,* 1992]. The four marine tephras (*L1–L4*) related to La Ese have volumes from 3 to 17.6 km^3 (*L1*= 8.4 km^3; *L2*= 5.2 km^3; *L3*=3 km^3; *L4*=17.6 km^3). Additionally, we can determine the first tephra volume for the

older (1.2 Ma) Caída Pumice fallout as 9 km^3, and the volume of the post-La Ese tephra layer *s13*, also from Guayabo caldera, as 6.4 km^3. In summary, eruptions from the Guayabo volcanic complex reached at least eruption magnitudes of M_V=5.5 to 6.3.

Units of the Liberia Formation below the Caída Pumice include the Buena Vista Ignimbrites (1.35 Ma; *Vogel et al.* [2004]), the Salitral Ignimbrite and the ~1.6 Ma old Liberia Tuff from the Cañas Dulces Caldera with its underlying Green Layer fallout [*Alvarado and Gans,* 2012]. We complement the cumulative volume of 7.75 km^3 [*Vogel et al.*, 2004] of the Buena Vista Ignimbrites on land by the volumes of the associated marine tephra layers (*N1*=6.6 km^3, M_V=5.8; *N2*=20.5 km^3, M_V=6.3; *N3*=19.1 km^3, M_V=6.3), as well as the volume of 14.95 km^3 of the Salitral Igbimbrite on land [*Chiesa et al.,* 1992], to obtain 68.9 km^3 of total erupted tephra volume. There are three marine tephra layers of a similar age range (*s19*=1.15 Ma, *s22*=1.32 Ma, *s23*=1.47 Ma), which originated from the northern part of the Guanacaste arc segment, and have tephra volumes (1.9–19.1 km^3) and eruption magnitudes (M_V=5.3–6.3) in the same range as the Buena Vista Ignimbrites.

Marine tephra layer *O* adds 48.6 km^3 to the minimum volume of 40 km^3 estimated for the Liberia Tuff on land [*Molina et al.*, 2014], so that the total 88.6 km^3 yield a magnitude of at least M_V=6.9. Including the volume of marine tephra *P* with that of the Green Layer results in a fallout tephra volume of 33.1 km^3 (M_V= 6.5) discharged immediately before the Liberia Tuff eruption. Clearly the Green Layer - Liberia was a very prominent event in the volcanic history of the Guanacaste segment. Two other, ~2 Ma old marine tephras, with typical compositions of the Cañas Dulces eruption products, represent smaller but still significant eruptive magnitudes (*s25*= 7.6 km^3, M_V= 5.9; *s26*= 6.1 km^3, M_V= 5.8).

The Bagaces Formation is the oldest described tephra sequence in the Guanacaste segment and consists of several individual ignimbrite layers that have been estimated to 100 ±40 km^3 erupted tephra volume in total [*Vogel et al.,* 2004; 2006; 2007]. In the marine record we found

distal facies of the well-known Cañas Ignimbrite (2.06 Ma; marine layer *Q*) and the Upper and Lower Sandillal Ignimbrites (4.1 and 4.15 Ma; marine layers *S* and *T*) [*Vogel et al.,* 2004; *Semm and Alvarado,* 2007, *Alvarado and Gans,* 2012], as well as 9 other tephra layers (*R1* to *R9*) that can be related to the Bagaces Formation. We combine volumes from ignimbrites mapped on land [*Semm and Alvarado,* 2007] with the distal volumes of the marine tephra layers and obtain 41.4 km^3 and 34.9 km^3 for the Upper and Lower Ignimbrites and 17.6 km^3 for the Cañas Ignimbrite, hence all in the range M_V= 6.3 to 6.6. Summing these volumes up with those of tephra layers *R1* to *R9* (3 to 24.7 km^3, M_V= 5.5 to 6.4), amount to a total tephra volume of 261 km^3 for the entire Bagaces Formation, more than twice the previous estimate.

For four widespread tephra layers (*s3*, *s9*, *s10*, *s15*) and four additional ash beds offshore Costa Rica that belong to the Las Sierras Formation in Nicaragua we determine tephra volumes from 1.1 to 5.1 km^3 (M_V= 5 and 5.7). These volumes lack the proximal on-land volume data, and thus are slightly lower than the new volume for the Fontana Tephra, which includes proximal data [*Wehrmann et al.,* 2006] and increases from 2.7 [*Kutterolf et al.*, 2008b] to 9.1 km^3 including the distal distribution offshore Costa Rica.

Two marine tephra layers (*G1, G2*) can be correlated to the Malpaisillo Caldera and roughly double the erupted tephra volume estimated by *Stoppa* [2015] from 5 to 8.3 km^3 for the Tolapa Tephra (*G1*, M_V= 5.9) and from ~3 to 5.1 km^3 for the La Fuente tephra (*G2*, M_V= 5.7).

Volumes from the older eruptions of the Coyol arc are difficult to determine since the exact location of the respective eruptive centers is not known. Nevertheless, assuming rough regions of origin for the individual eruptions results in erupted tephra volumes of 3 to 48 km^3, and respective eruption magnitudes of M_V= 5.5 to 6.7, considering only the distal tephra distribution in the Pacific.

The erupted magma masses (tables 1 and S2; typically on the order of 10^{12} to 10^{13} kg) corresponding to the individual tephra volumes are accumulated from old to young for each arc segment in Figure 6a. Changing slopes of the curves indicate significant temporal variations in long-term average eruption rates. The largest erupted mass per single event decreases continuously from the CCS ($2.6x10^{14}$ kg) to the GCS ($0.7x10^{14}$ kg), WNS ($0.7x10^{14}$ kg) and ENS ($0.3x10^{14}$ kg) segments (Table 1).. The eruptions with large erupted masses from the WNS are mostly eruptions of highly evolved magmas from the Coyol arc, located above thicker continental crust compared to ENS modern volcanic front data, possibly influencing magma evolution and storage behavior [e.g., *Leeman*, 1983; *Hildreth and Morbath*, 1988].

5 Discussion

5.1. Temporal and spatial variations of explosive arc volcanism

Several authors proposed periods of increased and decreased intensity of volcanic activity at the southern CAVA. *Carr et al.* [1982] for example identified periods of enhanced volcanism around 14 Ma, between 6 and 3 Ma, and within the last one million years. Significant lulls or gaps in between such periods are proposed by *Plank et al.* [2002], *Ehrenborg* [1996], and *Carr et al.* [2007] for Nicaragua between ~7 Ma and ~2 Ma after the southwest migration of volcanism from the Coyal arc to the modern volcanic front. *Carr et al.* [2007] even suggested that widespread volcanism does not appear to have resumed until ~600 ka to ~350 ka, the assumed age range of the beginning of the present volcanic arc front. *Saginor et al.* [2011a,b] modified these estimates and postulated a volcanic gap lasting from ~7 Ma to 3.6 Ma only, at least for the Western Nicaraguan segment.

In Costa Rica an extensive geochronologic survey of the Costa Rican volcanic belt by *Gans et al.* [2003] suggested several post-Miocene peaks of volcanic activity (6–4 Ma, 2–1 Ma, 600–400 ka and 100–0 ka) separated by apparent lulls. This has been modified by *Carr et al.* [2007], who identified continuous widespread eruptions between 1 Ma and recent.

Attempts, aiming to further fill these gaps in the volcanic record, are limited by the unfavorable preservation conditions (erosion, vegetation, superimposed younger deposits) and restricted to studies that sporadically fill parts of the gaps [e.g., *Alvarado and Gans,* 2012].

If we simply divide the marine ash beds of this study into two groups, of Costa Rican and Nicaraguan origin (Fig. 7), the resulting record for the last 8-9 M.y. is almost continuous, although a few apparent gaps of <1 M.y. duration appear. The Costa Rican record is continuous from 0 to 4 Ma with sporadic events back to 8 Ma (Fig. 7). For Nicaragua the marine tephra record suggests continuous large eruptions between ~9 Ma and 4 Ma as well as from ~1.7 Ma to recent time. Two tephras lie in the gap at ~3 Ma and 1.7 Ma (Fig. 7). Although several authors postulated a break in Nicaraguan volcanism when the westward shifting of the Neogene arc to the modern arc took place, we see no indication for a significant break in the explosive eruptive history. The first doubtless occurrence of modern arc volcanism at ~0.7 Ma is a marine ash layer (*s15*) that we correlate to the Las Sierras Formation. This ash layer thus implies an at least 100 kyr earlier begin of modern arc volcanism than previously estimated [*Carr et al.,* 2007]. Igneous rock compositions from Coyol and modern arcs can be distinguished by geochemical parameters indicating the influence of continental crust assimilation in the Coyol rocks [*Jordan et al.,* 2007a]. In the marine record, these geochemical characteristics (e.g., high La/Sm, Rb/Nd, Rb/Hf; see part 1) occur first at 1.54 Ma in Site U1414 (ash bed Interval *344-U1414A-14H-2, 71-75 cm*). Therefore we postulate that the shift from Coyol arc to modern volcanic front, evident in the related tephra deposits, occurred during the 1.54 to 0.7 Ma time window where we see no significant gap in activity (Fig. 7).

To elaborate more on temporal and spatial variations of the explosive southern Central American volcanism we compare the erupted magma masses from explosive volcanism per

segment along Costa Rica and Nicaragua for different time slices. The recorded magma mass of the Eastern Nicaraguan segment (ENS; $2.6x10x^{14}$ kg; Fig. 6a, b) was nearly exclusively produced within the interval 1-0 Ma (~$2.2x10x^{14}$ kg at an average magma flux of 0.052 g/m/s - normalized to segment length; the segment lengths are given in Table 1). On the Cordillera Central segment (CCS; $6x10^{14}$ kg and 0.126 g/m/s magma flux) half of the 1 to 0 Ma magma mass was produced during the eruption of the 322 ka Tiribí Tuff ($2.6x10^{14}$ kg). In contrast, in the neighboring Guanacaste segment (GCS) the erupted magma mass for the 1-0 Ma time slice ($8.8x10^{13}$ kg) and the corresponding magma flux (0.03 g/m/s) are small. However, the GCS stands out by the large magma mass erupted between 2-1 Ma ($3.6x10^{14}$ kg, Fig. 6a), a time interval when there was very little highly-explosive activity in the other segments. Moreover, these masses, emplaced as the rhyolitic Liberia Formation, were produced at an unusually large long-term magma flux of 0.125 g/m/s (Fig. 6a, Table 1). The erupted masses >3 Ma from the WNS (Coyol arc rhyolites) were produced at a much lower rate (0.035 g/m/s for the 4.5-7 Ma period; Fig. 6b, Table 1). Still lower magma production (0.02 g/m/s) governed the GCS during the 3-8 Ma period (Bagaces Formation rhyolites; Fig. 6a, Table 1).

These temporal changes may be interpreted to reflect as a lateral shift in the long-term magma eruption rates, but we emphasize that erupted magma masses that are discussed here, mainly relate to widespread tephra layers, because we lack consistent information on size and age of many older volcanic edifices and smaller-scale eruptions. This may be the reason why the Pliocene through Quaternary long-term average eruptive magma flux per arc length of ~0.017 g/m/s, obtained from the cumulative mass of $2.3x\ 10^{15}$ kg erupted along the 550 km of southern CAVA over the entire 8 Ma period, is only 40% the Late Pleistocene through Holocene (PH) flux (0.043 g/m/s) of *Kutterolf et al.* [2008b] and *Freundt et al.* [2014]. Another problem is the sampling bias that has to be considered, when comparing the data for the youngest time slice (<1 Ma) with the PH flux. For the WNS, which lies farthest away

from our drill locations, the <1 Ma flux of 0.019 g/m/s (Fig. 6a) is much smaller than the PH value of 0.046 g/m/s. This can be explained by the fact that the chance that fallout reaches a given location decreases with increasing distance from source. For the ENS, closer to our sampling sites, the discrepancy between 0.052 g/m/s (<1 Ma; Fig. 6a) and 0.08 g/m/s (PH value) is smaller. For both Nicaraguan arc segments however, we considered also the magma masses of the last 25 ka obtained by *Kutterolf et al.* [2008b], but these are mainly derived from eruptions of the ENS, which could explain the smaller discrepancy. At the Costa Rican arc segments the discrepancy reverses: 0.03 g/m/s (<1 Ma; Fig. 6a) versus only 0.0003 g/m/s (PH) for the GCS, and 0.126 g/m/s (<1 Ma; Fig. 6a) versus 0.083 g/m/s (PH) for the CCS. These relations result from the proximity of the segments to the drill sites and from the longer time interval (1 M.y.) compared to the former studies (~600 ka).

The following major conclusions can be derived from these observations:

1) For Costa Rica, there may be no apparent lulls in volcanism between 4 Ma and recent time, and 2) the Liberia Formation represents an unusually intense phase of volcanism on the GCS while at the same time (2-1 Ma) there was a lull in activity on all other arc segments. 3) For Nicaragua, if there is a volcanic gap at all it is limited to ~4 Ma to ~2 Ma, 4) this gap occurred at the Coyol arc and is apparently not related to the shift in arc position which happened at <1.54 Ma, 5) if this shift was associated with a break in volcanic activity it lasted less than ~800 kyr, 6) and the averaged eruptive mass flux from explosive volcanism is similar for the modern Nicaraguan volcanic front and the Pliocene Coyol arc (Fig. 6a). 7) In general, our data on erupted mass variation over time (Fig. 6b) supports the two phases of intense volcanic activity (1 to 0 and >3 Ma) in Central America proposed by *Carr et al.* [1982].

5.2. Variable Sedimentation rates

Incoming plate

Generally, the sedimentation rates are lower in the Pliocene/Early Pleistocene and increase toward Late Pleistocene and Holocene due to the approach of the Cocos plate to the Middle American trench, which caused an increasing flux of terrestrial matter onto the incoming plate. Further variability and hiatuses identified in the older incoming plate sediment sequences that deviate from the 1 to 5 m/M.y. sediment accumulation rates, typical for pelagic environments, can be explained by topographic features, e.g. the proximity to ocean islands. The overall higher sedimentation rates at Site 1241 may be a result of enhanced reworking, caused by the relatively rough relief of the Cocos Ridge. The peak sedimentation at 6-7 and 9-10 Ma (Fig. 3a) on the other hand may be explained by its position closer to the Galápagos Archipelago and incorporation of more volcaniclastics, which are visible in the sediments [*Mix et al.,* 2003]. The sediment record of Site 1242 is limited to the past 2 M.y. and thus entirely dominated by strong hemipelagic sedimentation close to the trench.

Pliocene to Late Miocene sediment hiatuses occur at Sites U1381 and 1242 although these are located next to Site U1414 that has a continuous and homogenous sedimentation. The causes for this discrepancy are subject of ongoing investigations [e.g., *Baxter et al.,* submitted]. Possible explanations are sought in the context of temporally and regionally variable interplays of erosion, morphology and biogenic productivity. Enhanced abrasion that removed 11-2 M.y. old sediments from Site U1381 within the Pliocene (Fig. 3a), may be attributed to the occurrence of strong bottom currents that could be related to the closure of the Panama isthmus (*Stone,* 2013). At the same time higher Pliocene sediment accumulation at Site U1414, at the footwall of the Cocos Ridge, may be explained by erosional detritus contribution from the Cocos Ridge. Similar Pliocene sedimentation rates occur at Site 1039, which was located in an open ocean environment at that time. However, the backtracked Pliocene position of Site 1039 was in the equatorial upwelling zone, which may be responsible for higher contents of siliceous microfossils reflecting higher Pliocene/Miocene productivity [e.g., *Mix et al.,* 2003] that may result also in an increase of the sedimentation

rate. However, more detailed investigations are required to shed light on the processes responsible for these inconsistencies [e.g., *Baxter et al.,* submitted].

Continental slope

Offshore Nicoya ,sedimentation rates of the last ~4 Ma show no significant changes with time at Sites 565, 1040 and 1041; only Site 1041 reaches farther back in time and shows an increase in the sedimentation rate at ~5 Ma. Unfortunately, the record ends and we have no evidence for the duration of this sedimentation pulse (number I in Figure 3b). In contrast, offshore Osa Peninsula sedimentation rates reached maximum values in the periods 0-0.2, 1.1–1.6 and around ~2.2-2.7 Ma (peaks of high sedimentation are numbered from IV-II in Figure 3 respectively). The recent sedimentation pulse IV is also visible at Sites U1414 and U1381 on the incoming plate, close to the trench. Sedimentation pulse III at around 1.5 Ma can be observed also at Site 1242 on the Cocos Plate, although at that time this position was about 100 km farther away from the trench, which would cause a decrease in the influx of terrigenous matter. Periodically enhanced sediment accumulation on the continental slope spilled over to the incoming plate sites, resulting in variable, mostly increased, sedimentation rates within the past 2.5 Ma.

The factors, which could be responsible for the episodic high to extremely high sedimentation rates at the slope offshore Osa Peninsula are 1) increased sediment flux as response to uplifted mountain ranges (Cordillera Talamanca or Fila Costeña; e.g., *Morell et al.* [2012]; *Morell* [2015]) in the hinterland of the Costa Rican shelf, due to subduction of seamounts/Cocos Ridge or, 2) episodic high subsidence rates of the forearc basin linked to subduction erosion processes providing the continuously deepening sediment trap to accumulate large packages of sediment.

5.3 Cocos Ridge arrival and subduction erosion

The time when the Cocos Ridge began to enter the Costa Rican subduction system is a matter of controversial discussion. Estimates ranging between ~1 Ma and the Miocene have been deduced from the emergence of the Osa Peninsula as well as uplift of the Cordillera de Talamanca and deformation of the Fila Costeña, tectonic reconstructions, and timing of arc volcanism [e.g., *Abratis and Woerner,* 2001; *Grafe et al.,* 2002; *Hey,* 1977; *Kolarsky et al.,* 1995; *Gardner et al.,* 1992; *Fisher et al.,* 2004; *MacMillian et al.,* 2004; *De Boer et al.,* 1995; *Lonsdale and Klitgord,* 1978; *Sutter,* 1985]. In principle, it should be possible to detect the arrival of the Cocos Ridge in the subduction system by changes in the geochemistry of the marine tephra layers as products of the arc volcanism (Fig. 8). In fact, compared to other CAVA volcanics the Central Costa Rican volcanic rocks feature a unique geochemical composition indicative of an OIB influence (e.g., low Ba/La, U/Th, Ba/Th, $^{143}Nd/^{144}Nd$, high La/Yb, $^{208}Pb/^{204}Pb$; e.g., *Hoernle et al.* [2008]; *Carr et al.* [2007]; *Herrstrom et al.* [1995]). However, there are several possibilities how these geochemical characteristics could have been achieved: 1) a residual Galápagos-type mantle remaining after the formation of the Caribbean Large Igneous Province (CLIP) [*Feigenson et al.,* 2004], 2) flow of OIB-type asthenospheric mantle from South America [*Herrstrom et al.,* 1995] to the region or a slab window [*Abratis and Wörner,* 2001], 3) subduction erosion of older accreted Galápagos and CLIP material from the upper plate in the Costa Rican fore-arc [*Goss and Kay,* 2006], and 4) subduction of the Galápagos hotspot track (e.g., Cocos Ridge) beneath Central Costa Rica since ~8 Ma [*Hoernle et al.,* 2008]. The geochemical signal is carried towards northwestern Nicaragua by arc-parallel mantle flow but diminishes by dilution with a "pure" Nicaraguan subduction component [*Hoernle et al.,* 2008]. *Goss and Kay* [2006] and *Hoernle et al.* [2008] associated a more radiogenic source evident in Pb-isotopes of southern Costa Rican and Panamanian volcanic rocks with the subduction of the Cocos Ridge and the erosion of the mafic forearc sediments within the last 6 Ma. *Clift et al.* [2005] explained temporally variable

OIB-like contributions in the compositions of the marine ash beds offshore Costa Rica by subduction erosion enhanced by the subduction of larger seamounts offshore Nicoya Peninsula.

There is a considerable time delay between the entry of the OIB material at the trench and the appearance of the OIB-signature in the arc magmas. This delay time can be estimated as 1.49±0.23 M.y. using the plate tectonic movement vectors (corrected velocity for obliquity Vc= 75.4±1.6 km/Ma) as well as the average subduction zone geometry for northern Costa Rica (depth to subducted slab below the arc H= 96.5±8 km, subduction angle of 58.9±4.6°) after *Syracuse and Abers* [2006]. The southern Costa Rican margin differs by a shallow subduction angle (20°) for the first 100 km and a subsequent very steep angle (~80°), where the shallow section is attributed to the subducting Cocos Ridge [e.g., *Dinc et al.*, 2010; *Dzierma et al.*, 2011; *Arroyo et al.*, 2014]. For these southern conditions, the time delay would be ~2±0.3 M.y., but we only use the value derived above because (1) it is uncertain when this modern subduction geometry has been established, (2) it is limited to the southern part of the Costa Rican subduction zone only, and (3) the difference between the two calculated times is small considering the uncertainties involved.

In absence of radiogenic isotope data for all tephra layers, we use trace element ratios indicative of an OIB-compositional signature in our marine tephras (e.g., Nb/Rb, Ba/La; Fig. 8a, b, e.g., *Herrstrom et al.* [1995]; *Willbold and Stracke* [2006]). Nb/Rb and Ba/La vary with SiO_2 such that the trace element ratios at >70 wt% SiO_2 are completely modified by fractional crystallization (Fig. 8c, d), e.g. the depletion of Rb by K-rich minerals. For the intermediate to mafic samples at <70 wt% SiO_2, however, the factor ~2 range in the trace element ratios at a given SiO_2 content (e.g., at 65 wt% SiO_2, Nb/Rb: 0.25 to 0.5 and Ba/La 18 to 38; Fig. 8c,d) cannot be explained by fractionation processes. We interpret these variations as changes in the magma sources involving variable contributions of OIB material.

In Figure 8 we show the temporal geochemical variation of marine tephras with an origin from Costa Rican volcanic complexes of the last 2 M.y.. In general, we observe a change with time and with the along arc provenance. Tephras from the Rincón, Miravalles/Guayabo and Tenorio volcanic complexes on the Guanacaste segment almost all have rhyolitic compositions with Nb/Rb<0.2 and Ba/La>30 (Fig. 8a, b) that are controlled by fractional crystallization. In contrast, the marine tephra layers from Barva volcano, and less so also those from Platanar and Poás volcanoes, which all lie on the Cordillera Central segment, have high Nb/Rb and low Ba/La ratios that we interpret as a strong OIB-signal (Fig. 8a, b). The maximum Nb/Rb values in the Barva data decrease, and the Ba/La values, slightly increase with time without any systematic decrease in SiO_2 with time (cf. Fig. S1); therefore the changes in the trace element ratios reflect a decrease in the OIB-signal with time (Fig. 8a, b). The first Barva ash bed featuring a significant OIB signal is ~1.42 Ma old (Interval *334-U1378B-36X-CC, 33-35 cm*). If we add the delay time 1.49±0.23 M.y. derived above, the corresponding introduction of OIB material into the subduction system must have occurred at 2.91±0.23 Ma.

We propose that this is the time when the thickened crust (~22 km; *Walther* [2003]) of the Cocos Ridge entered the trench. This hypothesis is supported by the fact that Barva, of all volcanic centers investigated here, lies closest to the inferred point of Cocos Ridge subduction beneath the Caribbean Plate [e.g., *Arroyo et al.*, 2014]. It also agrees with plate tectonic reconstructions by *MacMillan et al.* [2004] and *Morell et al.* [2011], which place subduction of the Panama Triple Junction near Osa Peninsula at 3 Ma just prior to Cocos Ridge subduction. Moreover, the other sources of an OIB signal introduced above (e.g., mantle flow, subduction erosion) have been operating over much longer times.

The peak II in sedimentation rate at >2.3 Ma (Fig. 3b) offshore Osa peninsula can then be explained by enhanced erosion of forearc regions, uplifted by the intruding Cocos Ridge. Ma

Moreover, *Vannucchi et al.* [2003, 2013] identified phases of subsidence and subduction erosion offshore Osa Peninsula at 2.3-2.2 Ma, as well as offshore Nicoya Peninsula at ~2.5 Ma, and these may also be related to tectonic deformation in the course of initial Cocos Ridge subduction considering the uncertainties in age constraints. A correlation between the onset of Cocos Ridge subduction and inner forearc uplift, however, cannot be simply made. Recent apatite fission track dating of the forearc sediments reveals that the granitoids of the Cordillera de Talamanca were unroofed <2.5 Ma, while the Fila Costeña started to develop <1.9 Ma [*Vannucchi et al.,* accepted], i.e. significantly later than initial Cocos Ridge subduction.

These tectonic conditions appear to have affected the arc volcanism. Possibly, due to compression by the Cocos Ridge, volcanism appears to have vastly diminished through the 3-1 Ma period on the CCS (Fig. 6b). On the other hand, the northerly adjacent GCS experienced an unusually productive phase of intense, large magnitude rhyolitic volcanism (Liberia Formation; Fig. 6a, b) that may have been fostered by crustal extension coupled to the compression at the Cocos Ridge entry zone to the south.

Other peaks in the sedimentation rate, identified in Figure 3, do not obviously relate to changes in volcanism. The peak I of higher sedimentation rate at ~5 Ma at Site 1041 (Fig. 3b) seems to be contemporaneous with a phase of subsidence at 6.5-5 Ma offshore Nicoya Peninsula [*Vannucchi et al.*, 2003, 2013]. Tephras derived from the GCS at that time are all rhyolitic (Bagaces Formation), therefore possible variations in an OIB-source component cannot be identified.

Presently, we cannot correlate the younger peaks III and IV (< 1.6 Ma) in sedimentation rates at Sites U1378, U1379, 1039, 1242, (Figs 2B, D, I, J, 3a, b) to specific events. However, the slope region between Nicoya and Osa peninsulas has been affected by subduction of seamounts that scatter the Cocos Plate seafloor north of the Cocos Ridge, and such subduction

causes local intense deformation at the continental slope [*Ranero and von Huene*, 2000]. At least five such seamounts subduction events occurred within the last 650 ka [*Hühnerbach et al.,* 2005]. We therefore propose that sedimentation events III and IV may have been caused by seamount subduction, rather than by large scaled subduction erosion. Further interpretations into the past, on the base of the available data for tephra composition and sedimentation rates, remain too speculative until new data are acquired.

6 Conclusions

We have shown that all widespread Neogene and Quaternary tephras that were emplaced at the investigated Pacific drill sites at their reconstructed positions were generated by Plinian and ignimbrite eruptions, that compare in magnitude to the range of the modern Mt. St. Helens (1981), Pinatubo (1991), and Tambora (1815) eruptions. The long-term rates of highly explosive volcanism vary regionally between arc segments, and with time on each segment; for Costa Rica these variations can be related to Cocos Ridge subduction. Previously proposed gaps or lulls in the volcanic activity of southern Central America are much shorter, more local or may not exist, and continuous eruption activity is indicated since at least ~4 Ma. .Notably the jump in volcanic activity from Coyol arc to modern volcanic front in Nicaragua, which our data places at 1.5-0.7 Ma, was apparently not associated with a major (>800 kyr) interruption in volcanism.

Marine sedimentation rates on the middle and lower continental slope reveal four periods of peak sedimentation, which can be related to subduction processes. The peak sedimentation at >2.3 Ma agrees well with initial subduction of the Cocos Ridge, which we infer at ~3 Ma, because it generated a geochemical OIB signal in arc magmatism that is first seen in Barva tephras at ~1.42 Ma, after about 1.5 M.y. of processing through the subduction system.

Acknowledgement

We thank K. Strehlow, I. Rohr and K. Fockenberg for sample preparation and M. Thöner, J. Fietzke, M. Frsiche, D. Rau, L. Bolge, F. Lin, Y. Chien and C. Hung for lab assistance. The Integrated Ocean Discovery Program provided shipboard data and samples. We kindly thank the German Research Foundation for funding this project (Ku-2685/2-1&2). Finally, we appreciate the reviews from R. v. Huene and an anonymous reviewer as well as the editorial handling of J. Feinberg.

References

Abratis, M., and Worner, G. (2001), Ridge collision, slab-window formation, and the flux of Pacific asthenosphere into the Caribbean realm, Geology, 29(2), 127-130.

Alvarado, G. E., and Carr, M. J. (1993), The Platanar-Aguas Zarcas volcanic centers, Costa Rica: spatial-temporal association of Quaternary calc-alkaline and alkaline volcanism, Bull. Volcanol., 55, 443-453.

Alvarado, G. E., and Gans, P. B. (2012), Síntesis geochronológica del magmatismo, metamorfismo y metalogenia de Costa Rica, América Central, Rev. Geol. Am. Cent., 46, 7-122.

Arroyo, I. G., Grevemeyer, I., Ranero, C. R., and von Huene, R. (2014), Interplate seismicity at the CRISP drilling site: The 2002 Mw 6.4 Osa Earthquake at the southeastern end of the Middle America Trench, Geochem. Geophys. Geosyst., 15(7), 3035-3050.

Barckhausen, U., Ranero, C. R., von Huene, R., Cande, S., and Roeser, H. (2001), Revised tectonic boundaries in the Cocos Plate off Costa Rica: Implications for the segmentation of the convergent margin and for plate tectonic models, J. Geophys. Res., 106(19), 207-220.

Bice, D. C. (1985), Quaternary volcanic stratigraphy of Managua, Nicaragua: correlation and source assignment for multiple overlapping plinian deposits, Geological Society of America Bulletin Geological Society of America Bulletin, 96(4), 553-566.

Carr, M. J., Rose, W. I., and Stoiber, R. E. (1982), Central America, Orogenic Andesite and Related Rocks, New York, Wiley, 149-166.

Carr, M. J. (1984), Symetrical and segmented variation of physical and geochemical characteristics of the Central American Volcanic Front, J. Volcanol. Geotherm. Res., 20, 231-252.

Carr, M.J., Feigensohn, M.D. and Benett, E.A. (1990), Incompatible element and isotopic evidence for tectonic control of source mixing and melt extraction along the central American arc, Contrib. Mineral. Petrol., 105, 369-380.

Carr, M.J., Saginor, I., Alvarado, G.E., Bolge, L.L., Lindsay, F.N., Milidakis, K., Turrin, B.D., Feigensohn, M.D. and Swisher III, C.C. (2007). Element fluxes from the

volcanic front of Nicaragua and Costa Rica, Geochem. Geophys. Geosyst., 8, doi:10.1029/2006GC001396.

Chiesa, S., Civelli, G., Gillot, P.-Y., Mora, O. and Alvarado, G.E. (1992), Rocas piroclásticas asociadas con La Formación de la Caldera de Guayabo, Cordillera de Guanacaste, Costa Rica. Rev. Geol. Amér. Central, 14, 59-75.

Clift, P. and Vannucchi, P. (2004), Controls on tectonic accretion versus erosion in subduction zones: Implications for the origin and recycling of the continental crust. Rev. Geophys., 42(2), doi: 10.1029/2003RG000127

Clift, P.D., Chan, L.H., Blusztajn, J., Layne, G.D., Kastner, M. and Kelly, R.K. (2005), Pulsed subduction accretion and tectonic erosion reconstructed since 2.5 Ma from the tephra record offshore Costa Rica. Geochem. Geophys. Geosys., 6(9), 1-21.

Cruciani, C., Carminati, E., and Doglioni, C. (2005), Slab dip vs. lithosphere age: No direct function, Earth. Planet. Sci. Lett., 238, 298-310.

De Boer, J. Z., Drummond, M. S., Bordelon, M. J., Defant, M. J., Bellon, H., and Mauri, R. C. (1995), Cenozoic magmatic phases of the Costa Rican island arc (Cordillera de Talamanca), in Mann, P., ed., Geologic and Tectonic Development of the Caribbean Plate Boundary in Southern Central America, Volume 295, 35-55.

DeMets, C. (2001), A new estimate for present-day Cocos-Caribbean plate motion: Implications for slip along the Central American volcanic arc, Geophys. Res. Lett., 28, 4043-4046.

Dinc, A. N., Koulakov, I., Thorwart, M. M., Rabbel, W., Flueh, E. R., Arroyo, I. G., Taylor, W., and Alvarado, G. (2010), Local earthquake tomography of central Costa Rica: transition from seamount to ridge subduction, Geophysical Journal International, 183(1), 286-302.

Dzierma, Y., Rabbel, W., Thorwart, M. M., Flueh, E. R., Mora, M. M., and Alvarado, G. E. (2011), The steeply subducting edge of the Cocos Ridge: Evidence from receiver functions beneath the northern Talamanca Range, south-central Costa Rica, Geochem. Geophys. Geosyst., 12(4), doi: 10.1029/2010GC003477

Ehrenborg, J. (1996), A new stratigraphy for the Tertiary volcanic rocks of the Nicaraguan highland, Geol. Soc. Am. Bull., 108, 830-842.

Feigenson, M. D., Carr, M. J., Maharaj, S. V., Bolge, L. L., and Juliano, S. (2004), Lead isotope composition of Central American Volcanoes: Influence of the Galápagos Plume., Geochem. Geoph. Geosy., 5(6), 1-14.

Fierstein, J., and M. Nathenson (1992), Another look at the calculation of fallout tephra volumes, Bull. Volcanol., 54, 156–167.

Fisher, D. M., Gardner, T. W., Sak, P. B., Sanchez, J. D., Murphy, K., and Vannucchi, P. (2004), Active thrusting in the inner forearc of an erosive convergent margin, Pacific coast, Costa Rica, Tectonics, 23(2), art. no.-TC2007, doi:10.1029/2002TC001464.

Freundt, A., Kutterolf, S., Schmincke, H. U., Hansteen, T. H., Wehrmann, H., Perez, W., Strauch, W., and Navarro, M. (2006), Volcanic hazards in Nicaragua: Past, present, and future., in Rose, W. I., Bluth, G. J. S., Carr, M. J., Ewert, J., Patino, L. C., and Vallance, J. W., eds., Volcanic hazards in Central America, Volume 412, Geol. Soc. Am. Spec. Publ., 141-165.

Freundt, A., Halama, R., Suess, E. und Völker, D. (2014), Introduction to the special issue on SFB 574 “Volatiles and fluids in subduction zones: climate feedback and trigger

mechanisms for natural disasters", Int. J. Earth Sci., 103(7), 1729-1731, doi: 10.1007/s00531-014-1059-9.

Gans, P.B., Alvarado-Induni, G., Perez, W., MacMillan, I., and Calvert, A. (2003), Neogene evolution of the Costa Rican arc and development of the Cordillera Central, Geological Society of America Abstracts with Programs, 35(4), http://gsa.confex.com/gsa/2003CD/fi nalprogram/abstract_51871.htm.

Gardner, T. W., Verdonck, D., Pinter, N. M., Slingerland, R., Furlong, K. P., Bullard, T. F., and Wells, S. G. (1992), Quaternary Uplift Astride the Aseismic Cocos Ridge, Pacific Coast, Costa-Rica, Geol. Soc. Am. Bull., 104(2), 219-232.

Goss, A. and Kay, S. (2006), Steep REE patterns and enriched Pb isotopes in southern Central American arc magmas: Evidence for forearc subduction erosion?, Geochem. Geophys. Geosyst., 7(5), doi: 10.1029/2005GC001163.

Grafe, K., Frisch, W., Villa, I. M., and Meschede, M. (2002), Geodynamic evolution of southern Costa Rica related to low- angle subduction of the Cocos Ridge: constraints from thermochronology, Tectonophysics, 348(4), 187-204.

Harris, R.N., Sakaguchi, A., Petronotis, K., and the Expedition 344 Scientists (2013), Proc. IODP, 344, College Station, TX (Integrated Ocean Drilling Program). doi:10.2204/iodp.proc.344.2013.

Hauff, F., Hoernle, K., Bogaard, P. V. D., Alvarado, G. E., and Garbe-Schönberg, D. (2000), Age and geochemistry of basaltic complexes in western Costa Rica: Contributions to the geotectonic evolution of Central America, Geochem. Geophys. Geosyst., 1(5), doi: 10.1029/1999GC000020.

Herrstrom, E.A., Reagan, M.K. and Morris, J.D. (1995), Variations in lava composition associated with flow of asthenosphere beneath southern Central America, Geology, 23, 617-620.

Hey, R. (1977), Tectonic evolution of the Cocos-Nazca spreading center, Geol. Soc. Am. Bull., 88, 1404-1420.

Hildreth, W., Moorbath, S. (1988), Crustal contributions to arc magmatism in the Andes of Central Chile, Contrib. Mineral. Petrol., 98, 455-489.

Hoernle, K., Abt, D., Fischer, K., Nichols, H., Hauff, F., Abers, G., Van den Bogaard, P., Heydolph, K., Alvarado, G., Protti, M., and Strauch, W. (2008), Arc-parallel flow in the mantle wedge beneath Costa Rica and Nicaragua, Nature, 451, 1094-1097.

Hühnerbach V, Masson DG, Bohrmann G, Bull JM, Weinrebe W (2005), Deformation and submarine landsliding caused by seamount subduction beneath the Costa Rican continental margin – new insights from high-resolution sidescan sonar data. In: Hodgson DM, Flint SS (eds) Submarine Slope Systems: Processes and Products, Geological Society of London, 244, 195-205.

Hüneke, H., and Mulder, T. (2011), Deep-Sea Sediments, Developments in Sedimentology, 63, Elsiever, New York. 849 p ISBN 978-0-444-53000-4

Jordan, B. R., Sigudsson, H., Carey, S. N., Lundin, S., Rogers, R., Singer, B., and Barguero-Molina, M. (2007a), Petrogenesis of Central American Tertiary ignimbrites and associated Caribbean Sea tephra, in Mann, P., ed., Geologic and Tectonic Development of the Caribbean Plate Boundary in Northern Central America, Volume GSA Special papers, Geological Society of Amercia, 115-179.

Jordan, B. R., Sigurdsson, H., Carey, S. N., Rogers, R., and Ehrenborg, J. (2007b), Geochemical variation along and across the Central American Miocene paleoarc in Honduras and Nicaragua, Geochim. Cosmochim. Acta, 71, 3581-3591.

Kandlbauer, J., and Sparks, R. (2014), New estimates of the 1815 Tambora eruption volume, J. Volcanol. Geotherm. Res., 286, 93-100.

Kempter, K.A., 1997, Geologic Evolution of the Rincón de la Vieja Volcano Complex, Northwestern Costa Rica [Ph.D.thesis]: Austin, Texas, University of Texas, 192 p.

Kimura, G., Silver, E. A., and Blum, P., et al. (1997), Proceedings ODP, Initial Reports, Volume 170, College Station, Texas, Ocean Drilling Program, 458p.

Klawonn, M., Houghton, B.F., Swanson, D.A., Fagents, S.A., Wessel, P., Wolfe, C.J. (2014), Constraining explosive volcanism: subjective choices during estimates of eruption magnitude, Bull. Volcanol., 76, 793, doi: 10.1007/s00445-013-0793-3

Kolarsky, R.A., Mann, P. and Montero, W. (1995) Island arc response to shallow subduction of the Cocos Ridge, Costa Rica. In: P. Mann (Editor), Geologic and tectonic development of the Carribean plate boundary, Geol. Soc. Am. Spec. Pap., 235-262.

Kutterolf, S., Freundt, A., and Peréz, W. (2008b), The Pacific offshore record of Plinian arc volcanism in Central America, part 2: Tephra volumes and erupted masses, Geochem. Geophys. Geosys., 9(2), doi:10.1029/2007GC001791.

Kutterolf, S., Freundt, A., Peréz, W., Mörz, T., Schacht, U., Wehrmann, H., and Schmincke, H.-U. (2008a), The Pacific offshore record of Plinian arc volcanism in Central America, part 1: Along-arc correlations, Geochem. Geophys. Geosyst., 9(2), doi:10.1029/2007GC001631.

Kutterolf, S., Freundt, A., Peréz, W., Wehrmann, H., and Schmincke, H.-U. (2007a), Late Pleistocene to Holocene temporal succession and magnitudes of highly-explosive volcanic eruptions in west-central Nicaragua, J. Volc. Geo. Res., 163, 55-82.

Kutterolf, S., Schacht U., Wehrmann H., Freundt A., Mörz T. (2007b), Onshore to offshore tephrostratigraphy and marine ash layer diagnesis in Central America. In: J. Buntschuh and G.E. Alvarado (eds) Central America - Geology, Resources and Hazards, Taylor & Francis /Balkema, ISBN-13:978-0-415-41648-1: 395-423.

Kutterolf, S., Freundt, A., Schacht, U., Bürk, D., Harders, R., Mörz, T., and Peréz, W. (2008c), The Pacific offshore record of Plinian arc volcanism in Central America, part 3: Application to forearc geology, Geochem. Geophys. Geosys., 9(2), doi:10.1029/2007GC001826.

Kutterolf, S., Liebetrau, V., Moerz, T., Freundt, A., Hammerich, T., and Garbe-Schönberg, D. (2008d), Lifetime and cyclicity of fluid venting at forearc mound structures determined by tephrostratigraphy and radiometric dating of authigenic carbonates, Geology, 36(9), 707-710.

Lallemant, H.G.A. (1996), Displacement Partitioning And Arc-Parallel Extension From the Southeastern Caribbean Plate Margin. In: G.E. Bebout, D.W. Scholl, S.H. Kirby and J.P. Platt (Editors), Subduction – Top to bottom. AGU Geophysical Monograph, 113-118.

Leeman, W.P. (1983), The influence of crustal structure on compositions of subduction-related magmas, J. Volcanol. Geotherm. Res., 18, 561-588.

Legros, F. (2000), Minimum volume of a tephra fallout deposit estimated from a single isopach, Journal of Volcanology and Geothermal Research, 96(1), 25-32.

Lonsdale, P., and Klitgord, K. D. (1978), Structure and tectonic history of the eastern Panama Basin, Geol. Soc. Am. Bull., 89, 981-999.

MacMillian, I., Gans, P. B., and Alvarado, G. (2004), Middle Miocene to present plate tectonic history of the southern Central American Volcanic Arc, Tectonophysics, 392(1-4), 325-348.

Mix, A.C., Tiedemann, R., Blum, P., et al. (2003), Proc. ODP, Init. Repts., 202, College Station, TX (Ocean Drilling Program), doi:10.2973/odp.proc.ir.202.2003

Molina, F., Martí, J., Aguirre, G., Vega, E., & Chavarría, L. (2014), Stratigraphy and structure of the Cañas Dulces caldera (Costa Rica). Geol. Soc. Am. Bull., 126(11-12), 1465-1480.

Morell, K. D., Fisher, D. M., Gardner, T. W., P., L. F., Davidson, D., and A., T. (2011), Quaternary outer fore-arc deformation and uplift inboard of the Panama Triple Junction, Burica Peninsula, J. Geophys. Res., 116, B05402, doi: 10.1002/2015GC005971

Morell, K.D., Kirby, E., Fisher, D.M. and van Soest, M. (2012), Geomorphic and exhumational response of the Central American Volcanic Arc to Cocos Ridge subduction, J. Geophysic. Res.: Solid Earth, 117(B4), doi: 10.1029/2011JB008969

Morell, K.D. (2015), Late Miocene to recent plate tectonic history of the southern Central America convergent margin. Geochem., Geophys., Geosys., 16(10), 3362-3382.

Morgan, J.P., Ranero, C.R. and Vannucchi, P. (2008), Intra-arc extension in Central America: links between plate motions, tectonics, volcanism, and geochemistry, Earth Planet. Sci. Lett., 272(1), 365-371.

Morris, J.D., Villinger, H.W., Klaus, A., et al., (2003). Proc. ODP, Init. Repts., 205: College Station, TX (Ocean Drilling Program). doi:10.2973/odp.proc.ir.205.2003

Münker, C., Wörner, G., Yogodzinski, G. and Churikova, T. (2004), Behaviour of high field strength elements in subduction zones: constraints from Kamchatka–Aleutian arc lavas, Earth Planet. Sci. Lett., 224(3), 275-293.

Newhall, C.G. and Self, S. (1982), The volcanic explosivity index (VEI): An estimate of explosive magnitude for historical volcanism. J. Geophys. Res., 87, 1231-1238.

Pérez, W., Alvarado, G. E., and Gans, P. B. (2006), The 322 ka Tiribí Tuff: Stratigraphy, geochronology and mechanisms of deposition of the largest and most recent ignimbrite in the Valle Central, Costa Rica, Bull. Volcanol., 69, 25-40.

Pérez, W., and Freundt, A. (2006), The youngest highly explosive basaltic eruptions from Masaya Caldera (Nicaragua): Stratigraphy and hazard assessment., in Rose, W. I., Bluth, G. J. S., Carr, M. J., Ewert, J., Patino, L. C., and Vallance, J. W., eds., Volcanic hazards in Central America, Volume 412, Geol. Soc. Am. Spec. Publ., 189-207.

Pisias, N.G., Mayer, L.A., Janecek, T.R., Palmer-JUlson, A. and von Andel, T.H. (Eds.) (1995), Proceedings ODP Scientific Results, 138, College Station, TX (Ocean Drilling Program).

Plank, T., Balzer, V., and Carr, M. (2002), Nicaraguan volcanoes record paleoceanographic changes accompanying closure of the Panama gateway, Geology, 30, 1087-1090.

Protti, M., Gundel, F., and McNally, K. (1995), Correlation between the age of the subducting Cocos plate and the geometry of the Wadati-Benioff zone under Nicaragua and Costa Rica., in Mann, P., ed., Geologic and Tectonic Development of the Caribbean Plate

Boundary in Southern Central America, Volume 295, Geol. Soc. Am. Spec. Pap, 309-326.

Pyle, D. M. (1989), The thickness, volume and grain size of tephra fall deposits, Bull. Volcanol., 51, 1-15.

Pyle, D.M. (1995), Mass and energy budgets of explosive volcanic eruptions, J. Geophys. Res. Let., 22(5), 563-566.

Pyle, D.M. (2000), Sizes of volcanic eruptions Encyclopedia. 263-270 pp; In: Sigurdson et al. Encyclopedia of Volcanoes, Academic Press, 1417 pp.

Ranero, C. R., and von Huene, R. (2000), Subduction erosion along the Middle America convergent margin, Nature, 404(6779), 748-752.

Ranero, C.R., von Huene, R. and Flueh, E. (2000), A cross section of the convergent Pacific margin of Nicaragua, Tectonics, 19(2), 335-357.

Rothwell, R.G. (2005), Deep Ocean Pelagic Oozes, Vol. 5. of Selley, Richard C., L. Robin McCocks, and Ian R. Plimer, Encyclopedia of Geology, Oxford, Elsevier Limited. ISBN 0-12-636380-3

Ryan, W.B.F., Carbotte, S.M., Coplan, J.O., O'Hara, S., Melkonian, A., Arko, R., Weissel, R.A., Ferrini, V., Goodwillie, A., Nitsche, F., Bonczkowski, J. and Zemsky, R. (2009), Global Multi-Resolution Topography synthesis, Geochem. Geophys. Geosyst., 10(3), doi: 10.1029/2008GC002332.

Saginor, I., Gazel, E., Carr, M. J., Swisher Iii, C. C., and Turrin, B. (2011a), New Pliocene-Pleistocene 40Ar/39Ar ages fill in temporal gaps in the Nicaraguan volcanic record, J. Volcanol. Geotherm. Res., 202(1), 143-152.

Saginor, I., Gazel, E., Carr, M. J., Swisher III, C. C., and Turrin, B. (2011b), Progreso y retos de la geocronología 40Ar/39Ar en Costa Rica y Nicaragua, Rev. Geol. Am. Central, 45, 75-86.

Schindlbeck, J. C., Kutterolf, S., Freundt, A., Straub, S. M., Wang, K.-L., Jegen, M., Hemming, S. R., Baxter, A. T., and Sandoval, M. I. (2015), The Miocene Galápagos ash layer record of Integrated Ocean Drilling Program Legs 334 and 344: Ocean-island explosive volcanism during plume-ridge interaction, Geology, 43(7), 599-602.

Semm, W. and Alvarado, G. E. (2007), Ignimbrites of the Pliocene Bagaces Formation near Caμas (Guanacaste, Costa Rica). N. Jb. Geol. Paläont., Abh., 246, 313-323; Stuttgart.

Sigurdsson, H. and Carey, S.N. (1989), Plinian and co-ignimbrite tephra fall from the 1815 eruption of Tambora volcano, Bull. Volcanol., 51, 243-270.

Stone, R. (2013), Battle for the Americas, Science, 341, 230-233.

Stoppa, L. (2015), Tephrachronostratigraphy of the Malpaisillo Caldera (Central-western Nicaragua), Master thesis, Université de Fribourg, 155pp.

Straub, S. M., Gomez-Tuena, A., Bindeman, I. N., Bolge, L. L., Brandl, P. A., Espinasa-Perena, R., Solari, L., Stuart, F. M., Vannucchi, P., and Zellmer, G. F. (2015), Crustal recycling by subduction erosion in the central Mexican Volcanic Belt, Geochim. Cosmochim. Acta, 166, 29-52.

Sutter, F.R. (1985), Sección geológica del Pacífico al Atlántico a través de Costa Rican, Rev. Geol. Am. Cent., 2, 23-32.

Syracuse, E. M., and Abers, G. A. (2006), Global compilation of variations in slab depth beneath arc volcanoes and implications, Geochem. Geophys. Geosys., 7(5), Q05017.

Tournon, J., and Alvarado, G. (1997), Mapa Geológico de Costa Rica, Scale, 1:500,000

Vannucchi, P., Scholl, D. W., Meschede, M., and McDougall-Reid, K. (2001), Tectonic erosion and consequent collapse of the Pacific margin of Costa Rica: Combined implications from ODP Leg 170, seismic offshore data, and regional geology of the Nicoya Peninsula, Tectonics, 20(5), 649-668.

Vannucchi, P., Ranero, C.R., Galeotti, S., Straub, S.M., Scholl, D.W. and McDougall-Ried, K. (2003), Fast rates of subduction erosion along the Costa Rica Pacific margin: Implications for non-steady rates of crustal recycling at subduction zones, J. Geophys. Res., 108(B11), doi:10.1029/2002/B002207.

Vannucchi, P., Galeotti, S., Clift, P., Ranero, C. and von Huene, R. (2004), Longterm subduction erosion along the Guatemalan margin of the Middle America Trench, Geology, 32, 617-620.

Vannucchi, P., Ujiie, K., Stroncik, N., and the Expedition 334 Scientists (2012), Proceeding IODP, Volume 334, Tokyo, Integrated Ocean Drilling Program Management International, Inc., doi:10.2204/iodp.proc.334.2012.

Vannucchi, P., Sak, P., Morgan, J.P., Ohkushi, K., Ujiie, K. and Scientists (2013), Rapid pulses of uplift, subsidence, and subduction erosion offshore Central America: Implications for building the rock record of convergent margins. Geology, 41(9), 995-998.

Vannucchi, P., Morgan, J.P., Silver, E.A. and Kluesner, J.W., (2016) Origin and dynamics of depositionary subduction margins. Geochem. Geophys. Geosystem., doi: 10.1002/2016GC006259.

Vannucchi, P., Morgan, J.P. and Balestrieri, M.L., Subduction erosion, and the de-construction of continental crust: the Central America case and its global implications. Gondwana Research, Accepted

Villegas, A. (2004), La formación alto palomo: flujos pumiticos de la cordillera volcanica central, Costa Rica. Revista Geológica de América Central, 30, DOI: http://dx.doi.org/10.15517/rgac.v0i30.7259.

Vogel, T. A., Patino, L. C., Alvarado, G. E., and Gans, P. B. (2004), Silicic ignimbrites within the Costa Rican volcanic front: Evidence for the formation of continental crust, Earth. Planet. Sci. Lett., 226, 149-159.

Vogel, T. A., L. C. Patino, J. K. Eaton, J. W. Valley, W. I. Rose, G. E. Alvarado, and E. L. Viray (2006), Origin of silicic magmas along the Central American volcanic front: Genetic relationship to mafic melts, J. Volcanol. Geotherm. Res., 156, 217–228.

Vogel, T., Patino, L., Alvarado, G.E., Rose, W.I. (2007), Petrogenesis of ignimbrites, in Bundschuh, J., and Alvarado, G. E., eds., Central America - Geology, Resources and Hazards, Volume 1, Lisse, Niederlande, Tokio, Japan, Balkema, 591-619.

von Huene, R. and Scholl, D.W. (1991), Observations at convergent margins concerning sediment subduction, subduction erosion, and the growth of the continental crust, Rev. Geophys., 29, 279-316.

Walther, C. H. (2003), The crustal structure of the Cocos ridge off Costa Rica, J. Geophys. Res.: Solid Earth, 108(B3), 2136, doi:10.1029/2001JB000888

Wehrmann, H., Bonadonna, C., Freundt, A., Houghton, B. F., and Kutterolf, S. (2006), Fontana Tephra: A basaltic plinian eruption in Nicaragua., in Rose, W. I., Bluth, G. J.

S., Carr, M. J., Ewert, J., Patino, L. C., and Vallance, J. W., eds., Volcanic hazards in Central America, Volume 412, Geol. Soc. Am. Spec. Publ., 209-223.

Wiesner, M. G., Wetzel, A., Catane, S. G., Listanco, E. L., and Mirabueno, H. T., (2004), Grain size, areal thickness distribution and controls on sedimentation of the 1991 Mount Pinatubo tephra layer in the South China Sea, Bull. Volcanol., 66, 226-242.

Willbold, M. and Stracke, A. (2006), Trace element composition of mantle end-members: Implications for recycling of oceanic and upper and lower continental crust, Geochem. Geophys. Geosyst., 7(4), Q04004.

Figure Captions

Figure 1. a) Overview map of Central America. Yellow and orange circles indicate drill site positions of deep-sea drilling programs. The black arrow indicates the direction of the Cocos Plate motion and relative velocity to the Caribbean Plate after *DeMets* [2001]. The four tectonic segments of Costa Rica and Nicaragua: WNS, ENS= Western and Eastern Nicaragua segments; GCS=Guanacaste segment, CCS=Cordillera Central segment. Inset: Map of Costa Rica and Nicaragua. MAT= Middle American Trench. Magenta circles show Late Pleistocene and Holocene eruption centers of the CAVA, green circles show old caldera structures along the arc. Maps created using GeoMapApp (http://www.geomapapp.org; GMRT-Global Multi-Resolution Topography; *Ryan et al.* [2009]).b) Seimic profile BGR99-44 showing the site locations of Leg 170 and 205 offshore Nicoya Peninsula (modified after *Morris et al.* [2003]). c) Line BGR99-7 showing the locations of Legs 334 and 344 drill sites offshore Osa Peninsula (modified after *Harris et al.* [2013]).

Figure 2. A) to J) show cumulative sediment thickness versus age for selected southern Central American drill sites (1241, 1242, 1040/1254/1255, 1039, 1041, 565, U1412, U1413, U1378 and U1379). Additional diagrams are given in *Baxter et al.* [submitted] (Sites U1381 and U1414). The slopes of line segments between independently dated tephras yield average sediment accumulation rates in m/M.y. These rates are plotted versus depth (mbsf) in the right diagrams. In (B) and (C) diagrams at the very right side are blown-up sections of the left diagrams. Red lines show age models derived in the respective initial reports by the shipboard parties, green lines are our new age models.

Figure 3. Sedimentation rates versus age of southern Central American drill sites. (a) incoming plate drill sites and core sections below the decollement at slope drill sites. (b) slope drill sites. Gray bars (numbers I-IV) highlight intervals with high sedimentation rates.

Figure 4. Isopach maps for all eruptions with more than one isopach including site to site correlations (*s20, s31, s27, s22, s14, s15, s18, s9, s19, s17, s13*) and correlations *D, H*, *N1, T, Q, O, L3, P, J, K1, L4, L1, L2, N2 and M*) as defined in part 1. All corresponding core intervals are provided in Table S3. Note that the shape of offshore isopachs is constrained by few available data only. Numbers along the arc indicate locations of Holocene eruption centers. Small black circles indicate drill site locations in the Pacific. Labeled large circles mark site locations traced back along then plate motion path in 1 M.y. steps in order to account for site migration since tephra emplacement.

Figure 5. Isopach thickness versus square root of isopach area plot of a) all tephra layers with correlations to specific deposits at the arc (*D, H*, *N1, T, Q, O, L3, P, J, K1, L4, L1, L2, N2 and M)*, and b) all marine site to site correlations (*s20, s31, s27, s22, s14, s15, s18, s9, s19, s17, s13)*. All isopach maps are shown in Figure 4. For detailed list of tephra intervals see Table

S3. Data for comparison for the 1815 Tambora eruption [*Kandlbauer and Sparks,* 2014], the 18th May 1981 Mt. St. Helens eruption [*Pyle,* 1989] and the 1991 Pinatubo eruption [*Wiesner et al.,* 2004].

Figure 6. (a) Minimum cumulative erupted magma masses for the tectonic segments of the southern CAVA. WNS= Western Nicaragua Segment, ENS= Eastern Nicaragua Segment, GCS=Guanacaste Segment, CCS=Cordillera Central Segment. Line slopes indicate average long-term mass eruption rates indicated as [g/m/s], i.e. normalized to segment length. See table 1 for listed data. b) Stacked-bar graph showing total erupted magma mass per age interval per tectonic segment. Colors identify time intervals.

Figure 7. Distribution over time of all tephra layers found within the last 8 Ma for Costa Rica and Nicaragua (data from Part 1).

Figure 8. Compositional variations a) Nb/Rb and b) Ba/La ratios of Costa Rican tephras over the last 2 M.y.. Arc, transional, and OIB ranges based on own data for the CAVA, *Willbold and Stracke* [2006], *Herrstrom et al.* [1995], and *Münker et al.* [2004]. c) Nb/Rb and d) Ba/La versus SiO_2 to show the effects of fractional crystallization (data from Part 1).

Figure S1. Compositional variation of SiO_2 over the last 2 M.y. (data from Part 1).

Figure 1.

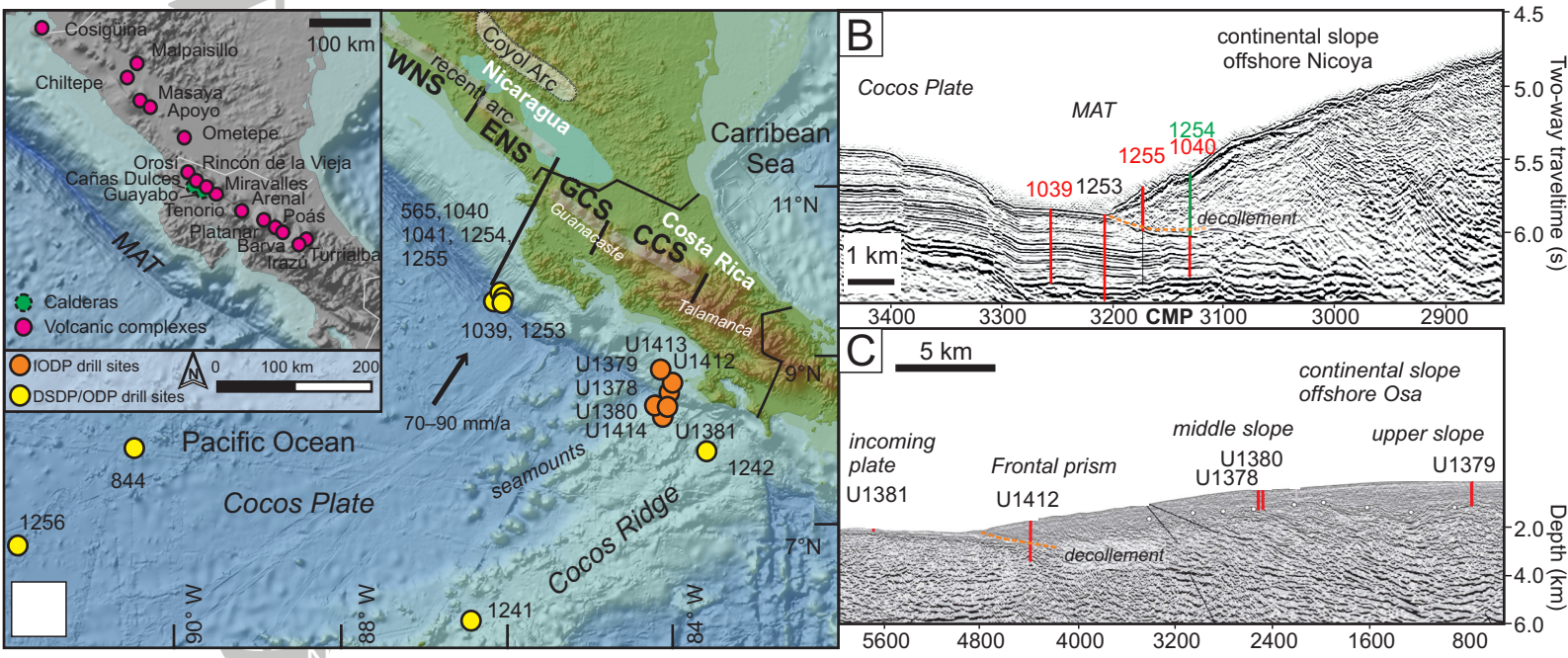

Figure 2.

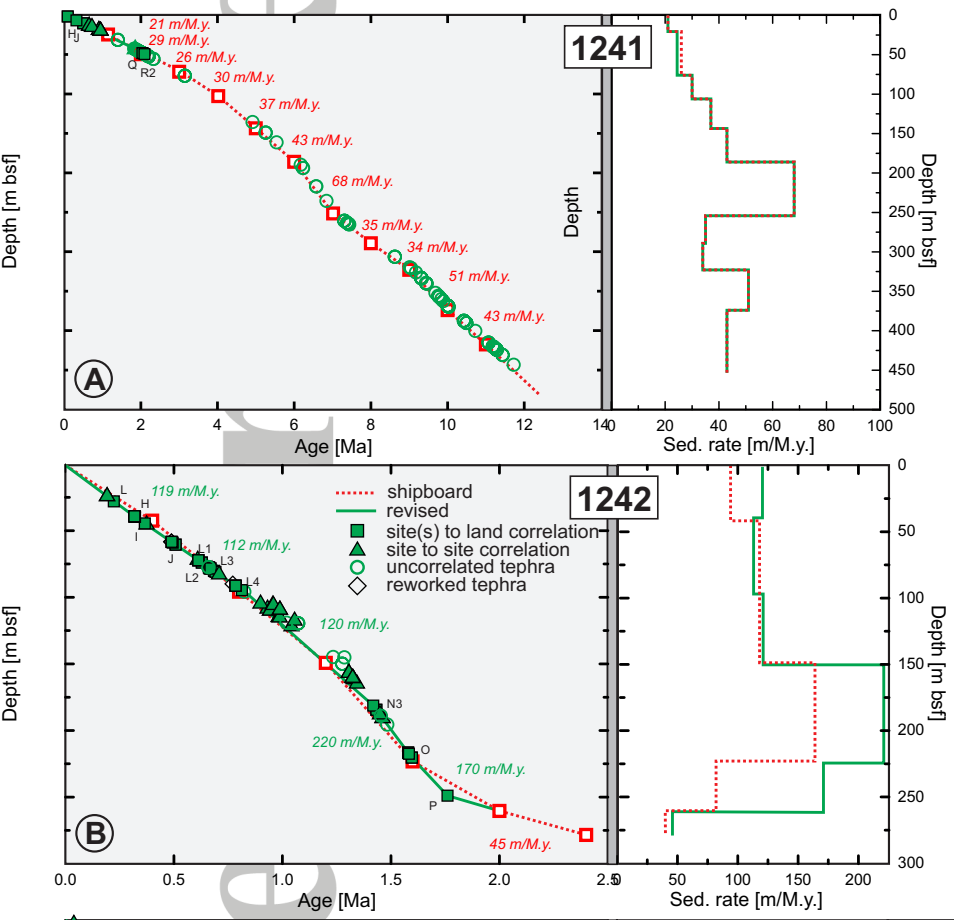

Tephras

A = Rincón de la Vieja Tephra; 3.5 ka
B = Terra Blanca 4; 36 ka
C1 = Poás ~40 ka
C2 = Poás Lapilli Tuff; >40 ka
D = Fontana Tephra; ~60 ka
E = Los Chocoyos; 84 ka
F = L-Fall Tephra; 191 ka
G = Tolapa Tephra; ~300 ka
H = Tiribí Tuff; 322 ka
I = Upper Canal/Tenorio Ignimbrite; ~450 ka*
J = Bajo La Hondura Tuff; 500 ka
K1 = Upper Alto Palomo Tuff; 520 ka
K2 = Lower Alto Palomo Tuff; 580 ka
L1 =Upper La Ese Ignimbrite; 634 ka
L2 =Upper La Ese Ignimbrite; 652 ka
L3 =Upper La Ese Ignimbrite; 665 ka
L4 =Lower La Ese Ignimbrite; 890 ka
M = Caída Pumice; 1.18 Ma
N1 = Buena Vista Ignimbrite; 1.25 Ma*
N2 = Buena Vista Ignimbrite ; 1.31 Ma
N3 = Buena Vista Ignimbrite; 1.456 Ma
O = Liberia Tuff; 1.595 Ma
P = Green Layer; ~1.7 Ma*
Q = Cañas Ignimbrite; 2.06 Ma
R2 = Bagaces Formation; ~2.3 Ma*
R4 = Bagaces Formation; ~2.8 Ma*
S = Upper Sandillal Ignimbrite; 4.1 Ma
T = Lower Sandillal Ignimbrite; 4.15 Ma

* av. age from site to site correlation

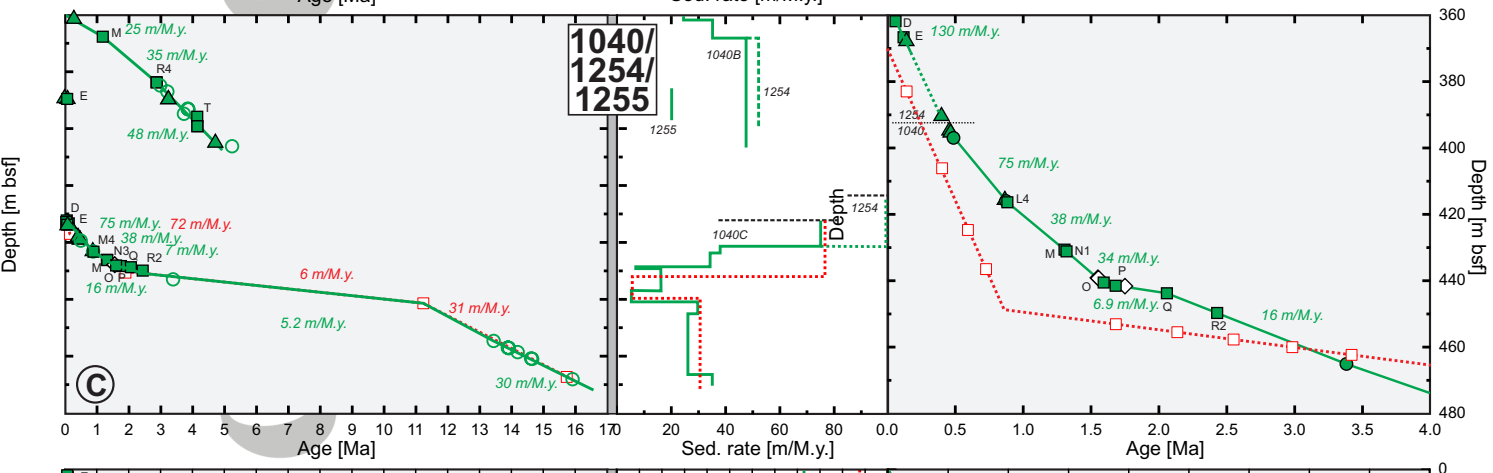

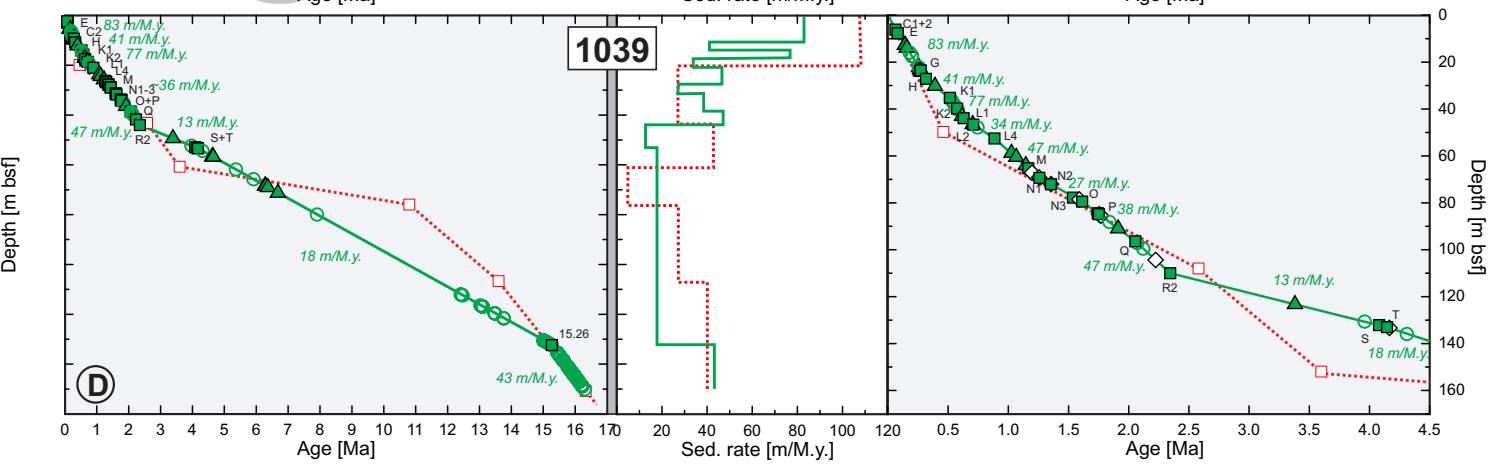

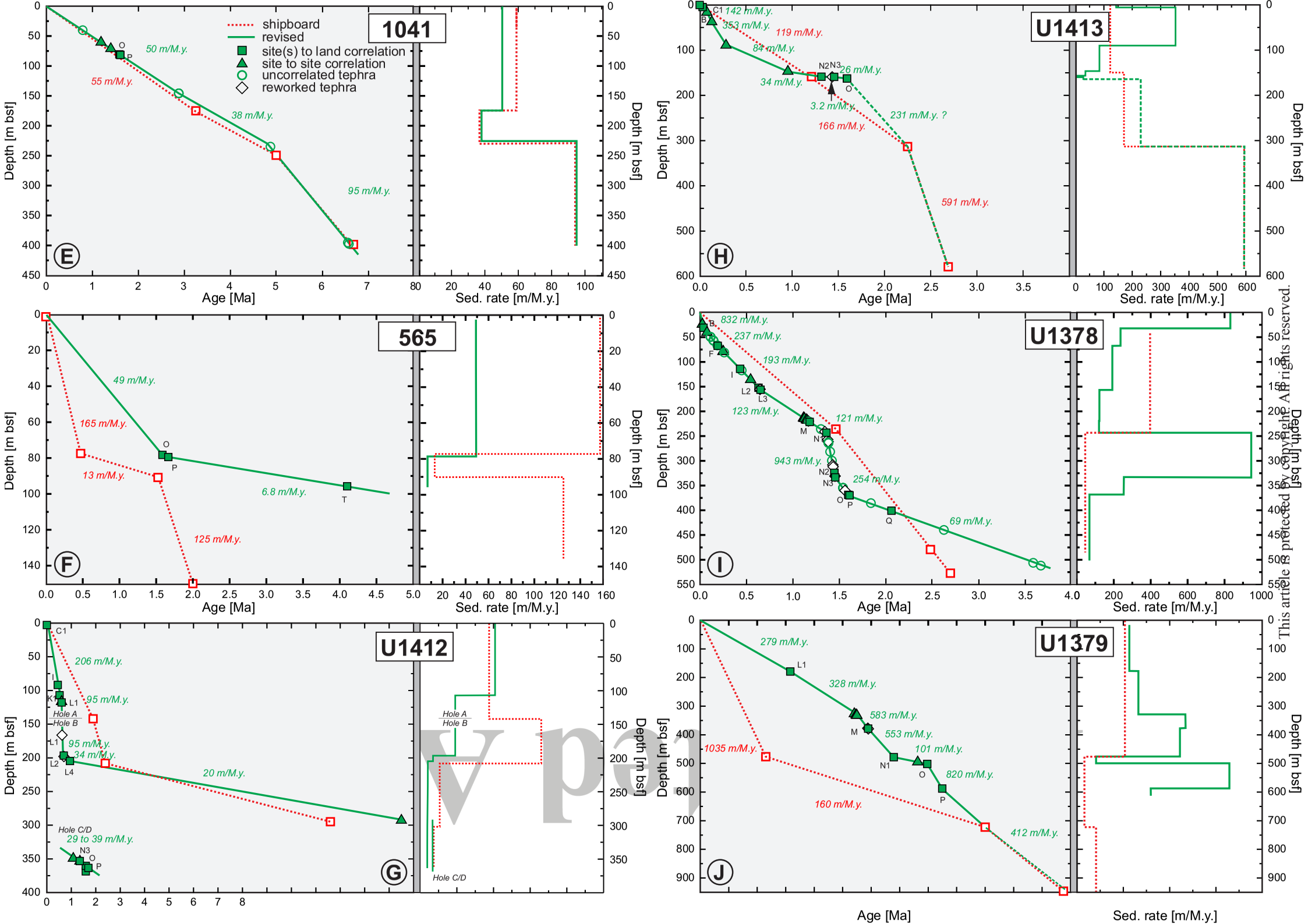

Figure 3.

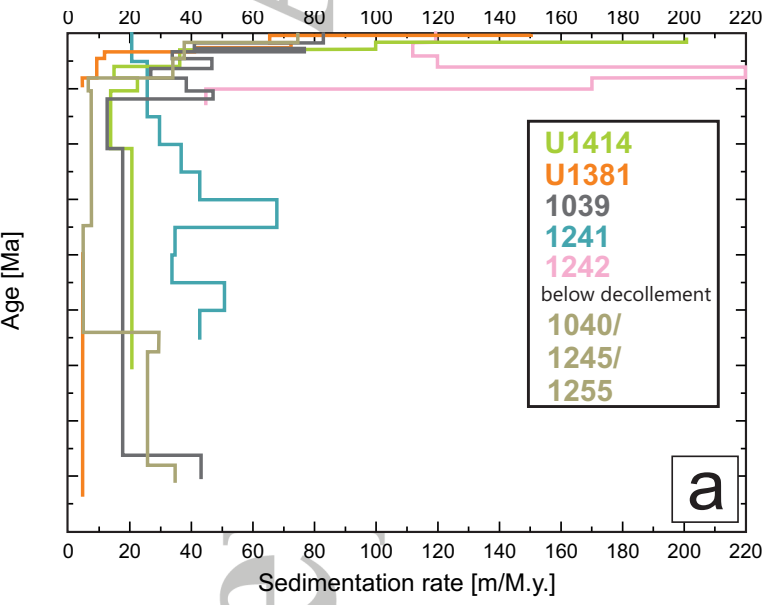

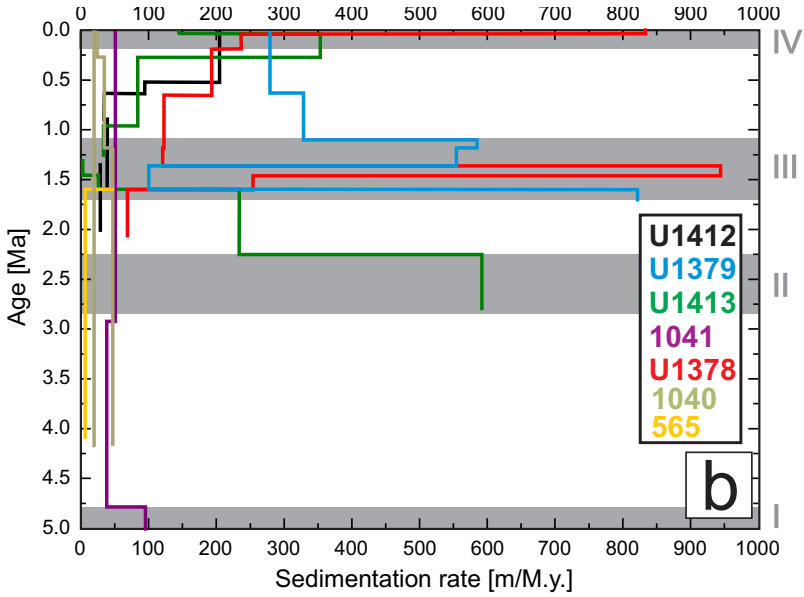

Figure 4.

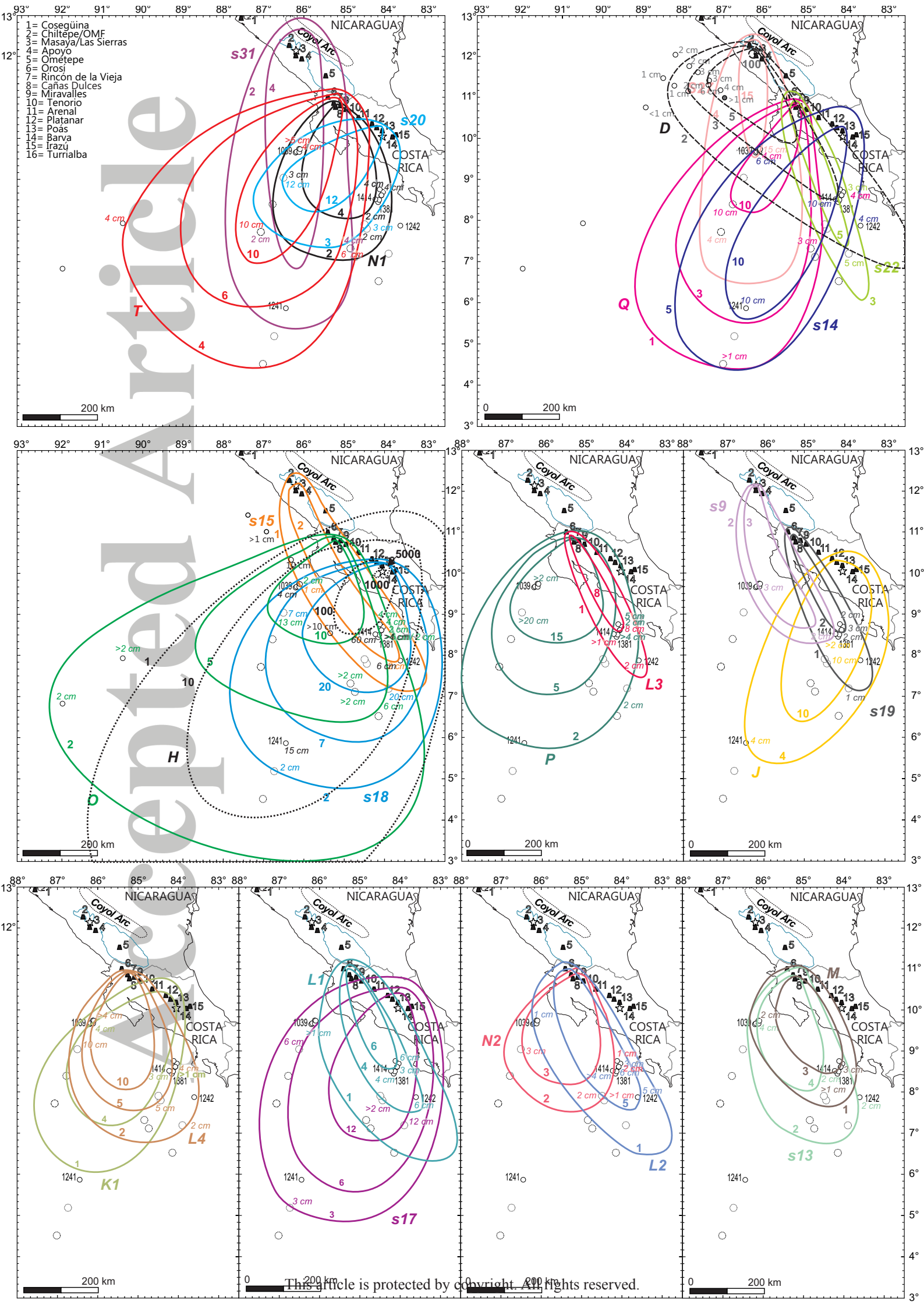

Figure 5.

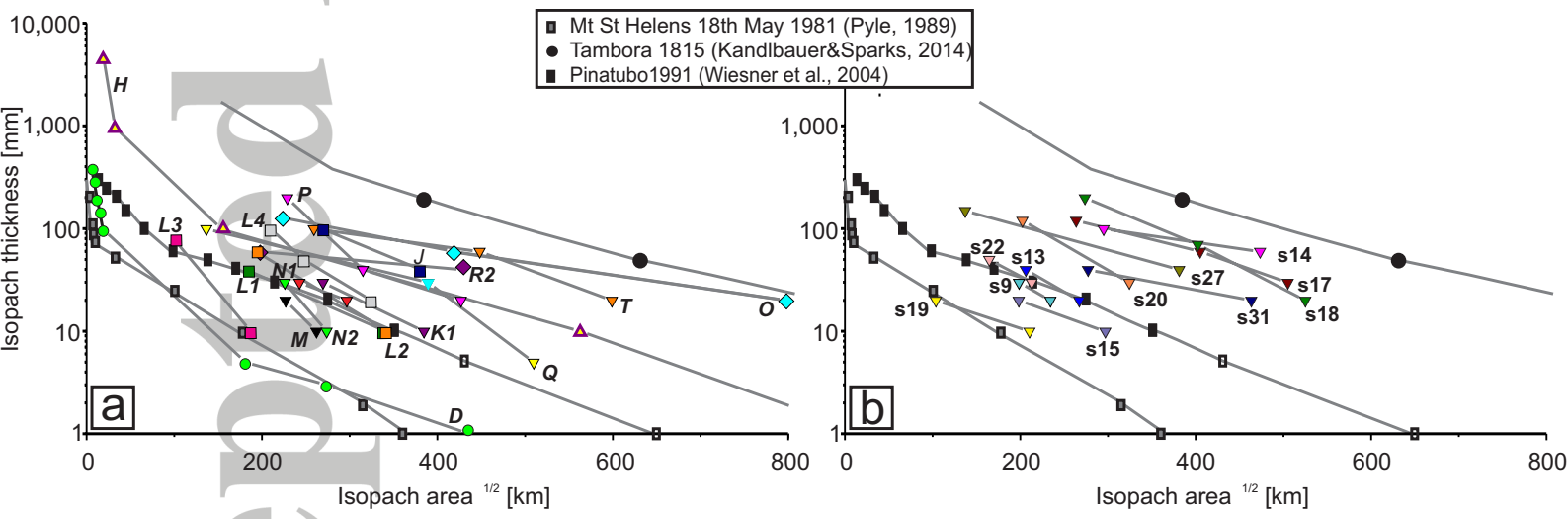

Figure 6.

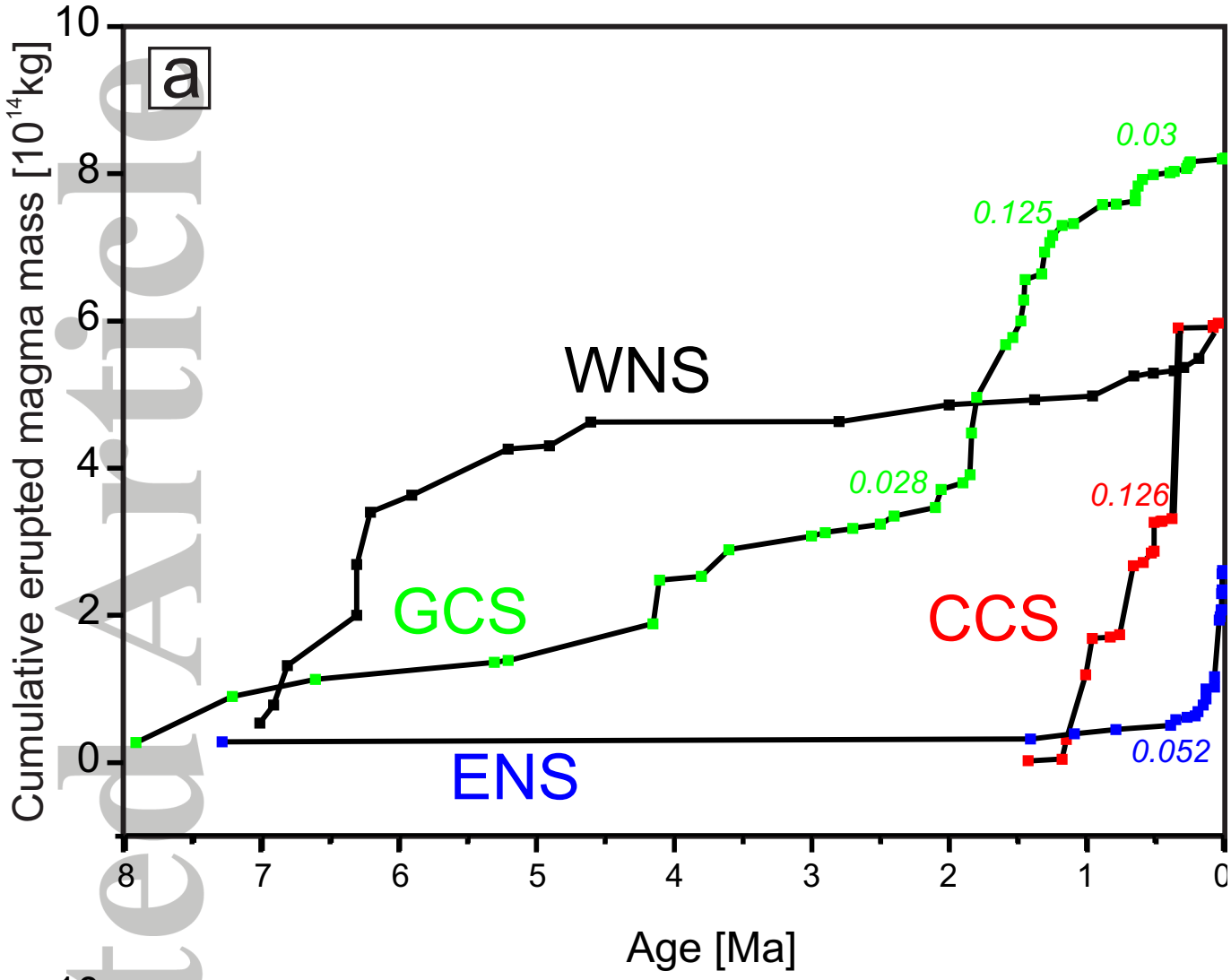

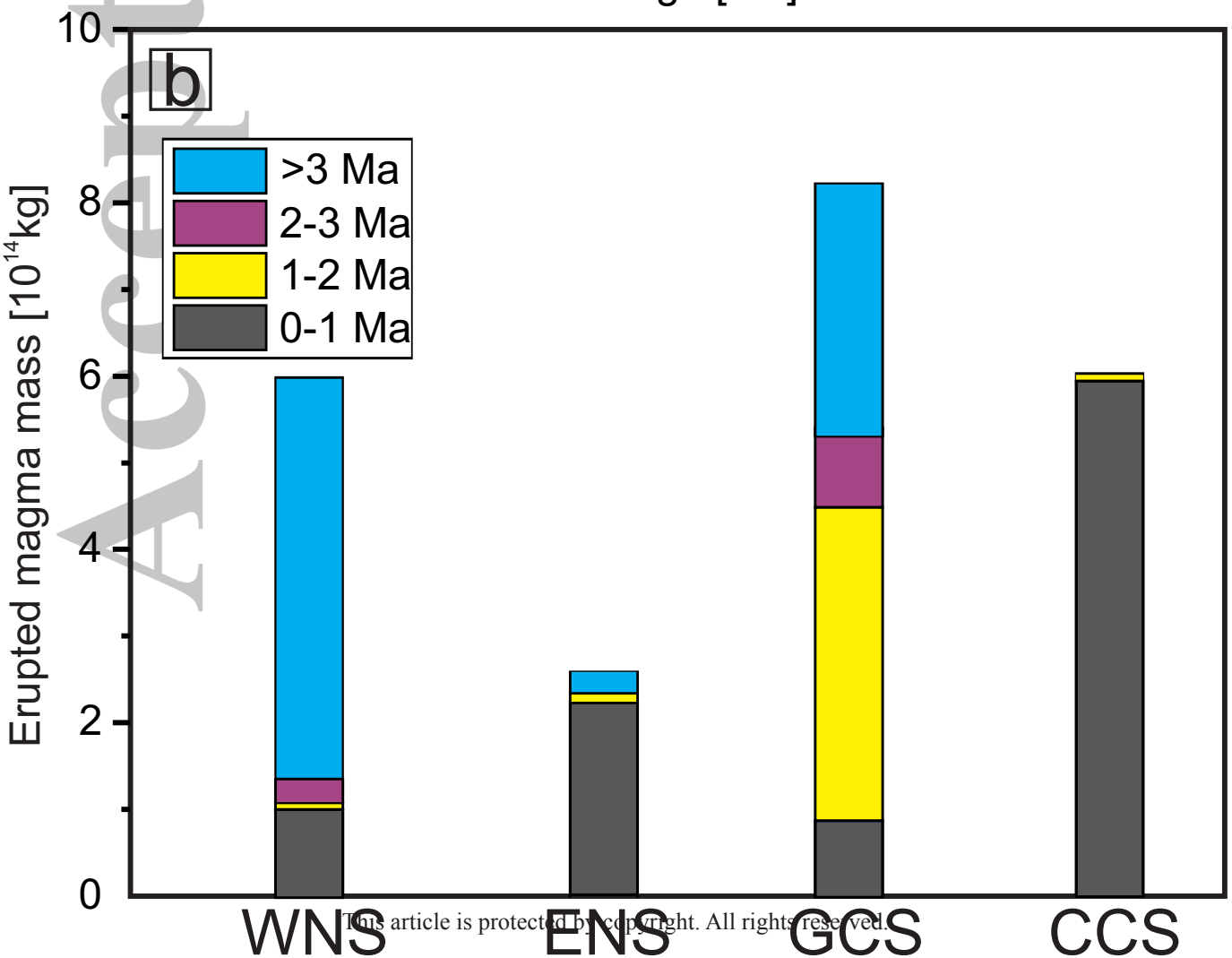

Figure 7.

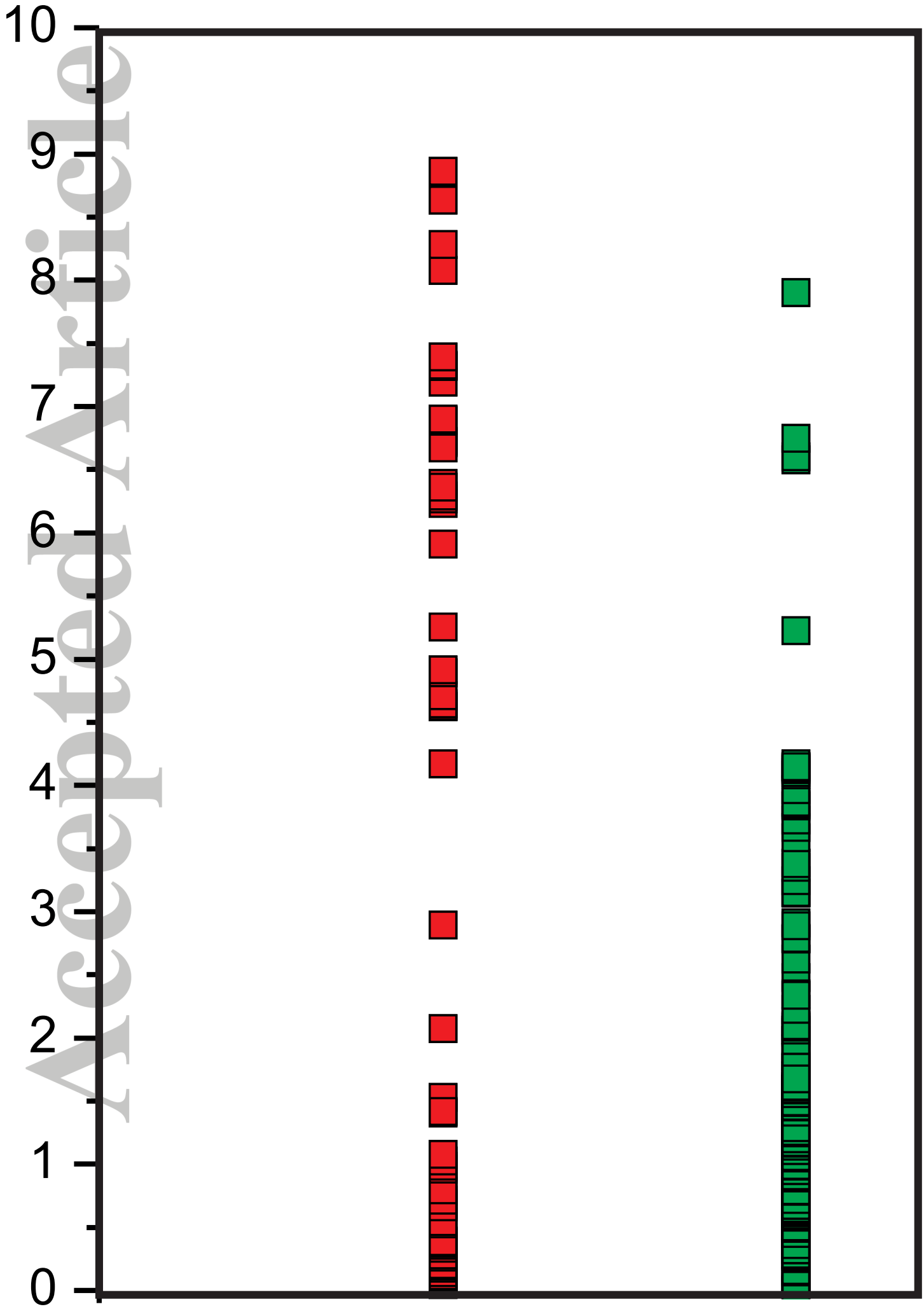

Figure 8.

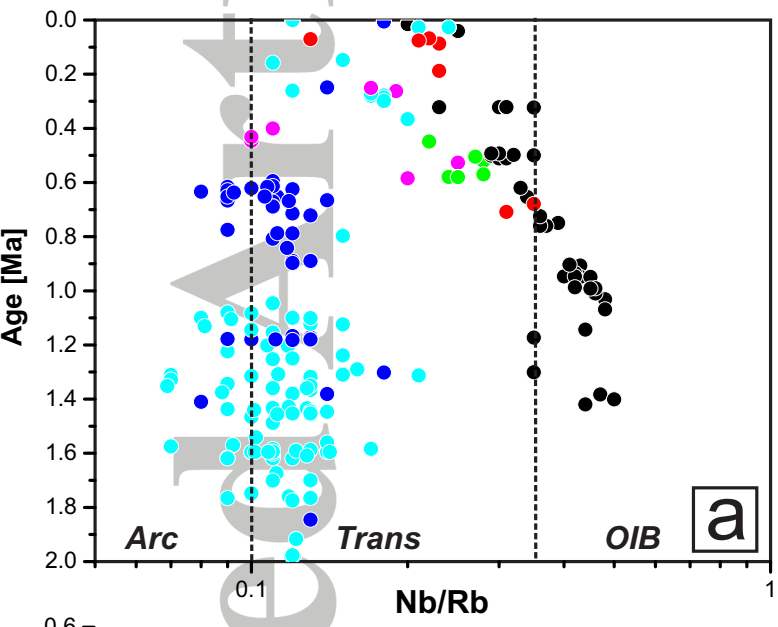

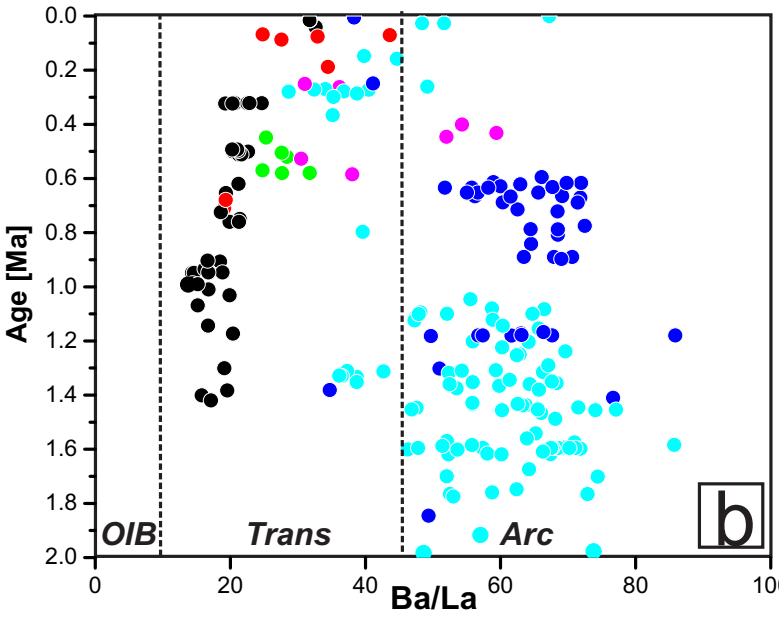

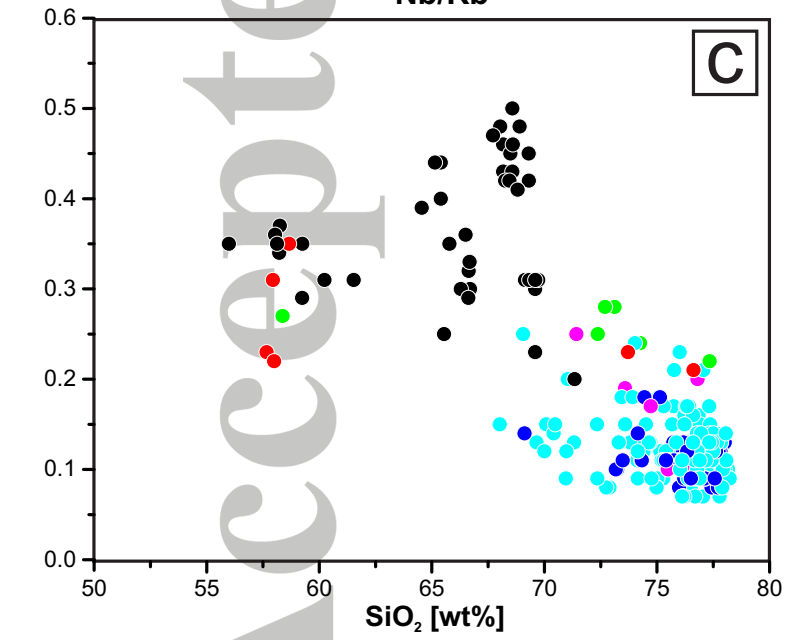

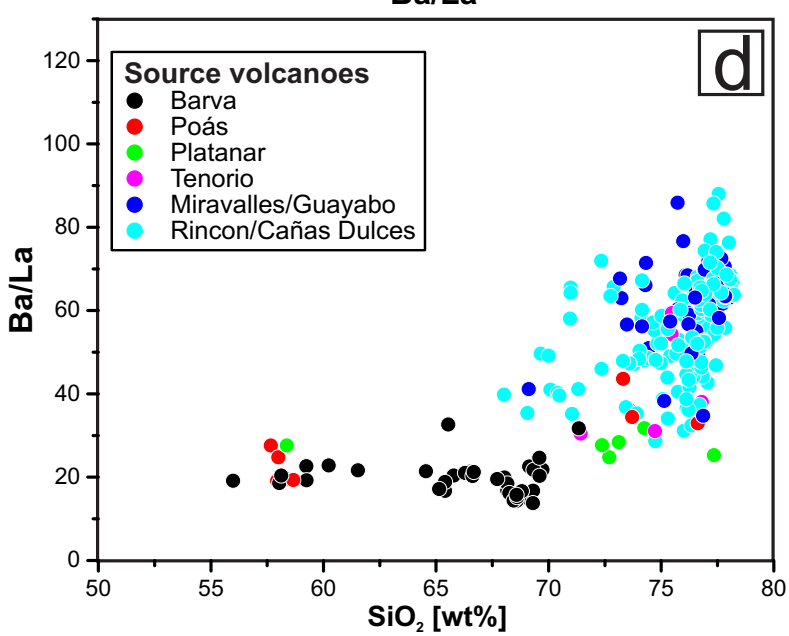

Table 1:Temporal tephra magma flux per segment.

Segment	segment age/duration	segment length (km)	Tephra mass (kg)	magma flux (g/s)	flux per length (g/m/s)
Western Nicaraguan segment*		166	8.48E+13	7679	0.046
WNS 0-1 Ma	1000000	166	1.02E+14	3225	0.019
WNS 1-2 Ma	1000000	166	7.42E+12	235	0.001
WNS 2-3 Ma	1000000	166	2.35E+13	743	0.004
WNS >3 Ma	4000000	166	4.61E+14	3652	0.022
WNS >1 Ma	6000000	166	4.92E+14	2598	0.016
Total	**7000000**	**166**	**5.94E+14**	**2687**	**0.016**
Eastern Nicaraguan segment*		137	1.20E+14	10899	0.080
ENS 0-1 Ma	1000000	137	2.23E+14	7066	0.052
ENS 1-2 Ma	1000000	137	1.13E+13	357	0.003
ENS 2-3 Ma	1000000	137			
ENS >3 Ma	4500000	137	2.68E+13	189	0.001
ENS >1 Ma	6500000	137	3.81E+13	186	0.001
Total	**7500000**	**137**	**2.61E+14**	**1103**	**0.008**
Guanacaste segment*		92	5.00E+11	26	0.0003
GCS 0-1 Ma	1000000	92	8.83E+13	2799	0.030
GCS 1-2 Ma	1000000	92	3.62E+14	11457	0.125
GCS 2-3 Ma	1000000	92	8.14E+13	2581	0.028
GCS >3 Ma	5000000	92	2.91E+14	1844	0.020
GCS >1 Ma	7000000	92	7.34E+14	3323	0.036
Total	**8000000**	**92**	**8.22E+14**	**3257**	**0.035**
Cordillera Central segment*		150	2.37E+14	12509	0.083
CCS 0-1 Ma	1000000	150	5.95E+14	18866	0.126
CCS 1-2 Ma	500000	150	3.25E+12	206	0.001
CCS 2-3 Ma	1000000	150			
CCS >3 Ma	1000000	150			
CCS >1 Ma	500000	150	3.25E+12	206	0.0014
Total	**1500000**	**150**	**5.99E+14**	**12646**	**0.084**
Sum S-CAVA* 600 ka	600000	545	4.43E+14	23373	0.043
Sum S-CAVA	**8000000**	**545**	**2.28E+15**	**9019**	**0.017**
Sum Neogene S-CAVA	**7000000**	**545**	**1.27E+15**	**5743**	**0.011**
Sum 0-1 Ma	**1000000**	**545**	**1.01E+15**	**31957**	**0.059**

***Freundt et al.* [2014]**